



UNIVERSITY OF IOANNINA
Department of Medicine
Department of Chemistry Department of Biological Applications and Technology

BIOMEDICAL RESEARCH INSTITUTE (BRI), FOUNDATION FOR RESEARCH AND
TECHNOLOGY-HELLAS (FORTH), IOANNINA ,GREECE

Interdisciplinary Postgraduate Program “Molecular-Cellular Biology and
Biotechnology”

Master’s thesis:

A 2D human iPSC-derived culture model to study sensory dysfunction in
neurodevelopmental disorders.

By Pothos Panagiotis,

Biologist, Bsc, Msc

Supervisor: CHRISTOS GKOGKAS, PhD

Researcher A’, BRI, FORTH, Ioannina

Acknowledgements

The present Thesis was carried out at the Institute of Biomedical Research Institute (BRI) - Foundation for Research and Technology-Hellas (FORTH). This thesis completes my MCs studies in the University of Ioannina.

I would like to express my sincere gratitude to my thesis advisor, Dr, Christos Gkogkas, for their invaluable guidance, support, and encouragement throughout the entire research process. Their expertise and insights significantly contributed to the development and completion of this thesis.

I am thankful for the support of my committee members, Dr. Stathis Friligos, Dr. Thomais Papamarkaki, Dr. Micaela Filiou, Dr. Giorgos Leodarithis for the knowledge they imparted to me in the postgraduate courses and all the professors of my master's program.

I am indebted to my colleagues in the lab Dr Klairi Xalkiadaki, Elpida Statoula, Maria Zafiri who generously shared their knowledge and experiences, enriching the discussions and shaping the ideas presented in this thesis.

Heartfelt thanks to my family for their unwavering support, understanding, and patience during the challenging moments of this academic journey.

Thank you all for being an integral part of this journey.

Abstract

Autism spectrum disorders are neurodevelopmental disorders related to changes in social behavior, repetitive stereotypical behaviors, and restricted interests. They affect 1 in 60 children. 95% of individuals with ASD experience sensory disorders. These individuals show increased sensitivity to touch/mechanical stimuli and thermal pain. This phenomenon of tactile hypersensitivity can contribute to the avoidance of social contact, resulting in the impaired functioning of the individual. The sense of touch is mediated by mechanoreceptors whose endings are located on the skin. Mechanoreceptors belong to the family of sensory neurons. Sensory neurons are pseudo-unipolar neurons where one end is connected to the central nervous system, and the other end is in the body's periphery to convey information to the central nervous system, specifically to the brain. Studies have shown that rodents with autism-related gene deletions exhibit tactile hypersensitivity, hyperactivation of mechanoreceptors, leading to behaviors associated with ASD. The proposed mechanism behind this phenomenon involves the mTOR pathway. Hyperactivation of mTORC1 in sensory neurons results in changes in general and specific protein synthesis, increased excitability of peripheral sensory neurons (e.g., touch), changes in the transmission and processing of sensory information in the CNS. This sequence of events leads to deficits and other behaviors associated with the autism spectrum. The specific purpose of this study was to differentiate and develop sensory neurons in vitro, specifically mechanoreceptors, from iPSCs (induced pluripotent stem cells).

Our results showed that with the protocol used for the differentiation and development of sensory neurons, we successfully generated sensory neurons that express key markers of 'sensory fate', such as TrkA, TRkB, TrkC. Furthermore, we investigated markers more specific to a subtype of sensory neurons, such as RunX1. Additionally, to monitor their development, we used markers such as pax6, nestin, tuJ1, MAP2. Finally, a study was conducted on the expression of Piezo2, a characteristic marker expressed in mechanoreceptors.

Περίληψη

Οι διαταραχές αυτιστικού φάσματος είναι νευροαναπτυξιακές διαταραχές οι οποίες σχετίζονται με αλλαγές στην κοινωνική συμπεριφορά, επαναλαμβανόμενες στερεοτυπικές συμπεριφορές και περιορισμένα ενδιαφέροντα και εμφανίζονται σε 1 στα 60 παιδιά. Το 95% των ατόμων με ASD εμφανίζουν αισθητηριακές διαταραχές. Τα άτομα αυτά εμφανίζουν αυξημένη ευαισθησία στο άγγιγμα/μηχανικό ερέθισμα και θερμικό πόνο. Το φαινόμενο αυτό της απτικής υπερευαισθησίας μπορεί να συμβάλει στην αποφυγή της κοινωνικής επαφής, με αποτέλεσμα την κανονική δυσλειτουργία του ατόμου. Η αίσθηση της αφής δημιουργείται από τους μηχανοϋποδοχείς που οι απολήξεις τους καταλήγουν πάνω στο δέρμα. Οι μηχανοϋποδοχείς ανήκουν στην οικογένεια των αισθητήριων νευρώνων. Οι αισθητήριοι νευρώνες είναι ψευδοδιπολικοί νευρώνες όπου το ένα τους άκρο συνδέεται στο κεντρικό νευρικό σύστημα, και το άλλο βρίσκεται στην περιφέρεια του σώματος για να εισέρχονται οι πληροφορίες στο κεντρικό νευρικό σύστημα κατά επέκταση του εγκεφάλου. Έχειδειχθεί ότι σε ποντίκια που είχε γίνει απαλοιφή γονιδίων που σχετίζονται με τον αυτισμό παρουσίαζαν απτική υπερευαισθησία. Υπερδιέγερση των μηχανοϋποδοχέων τους είχε ως αποτέλεσμα συμπεριφορές που σχετίζονται με ASD. Ο μηχανισμός που εικάζεται ότι βρίσκεται πίσω από αυτό το φαινόμενο είναι στο μονοπάτι του mTOR. Γίνεται υπερενεργοποίηση της κινάσης mTORC1 σε αισθητηριακούς νευρώνες που επιφέρει αλλαγές στην γενική και ειδική πρωτεϊνσύνθεση, αυξημένη διεγερσιμότητα των περιφερειακών αισθητήριων νευρώνων (π.χ. αφής), αλλαγές στην μετάδοση και επεξεργασία αισθητηριακών πληροφοριών στο ΚΝΣ, όπου η αλληλουχία αυτή γεγονότων επιφέρει ελλείμματα και άλλες συμπεριφορές που σχετίζονται με το φάσμα του αυτισμού. Ο σκοπός της συγκεκριμένης εργασίας ήταν η διαφοροποίηση και η ανάπτυξη των αισθητήριων νευρώνων *in nitro*, και πιο συγκεκριμένα μηχανοϋποδοχέων από iPSCs.

Τα αποτελέσματα μας έδειξαν ότι μετά το πρωτόκολλο που χρησιμοποιήσαμε για την διαφοροποίηση και την ανάπτυξη των αισθητήριων νευρώνων είχαμε δημιουργήσει πράγματι αισθητήριους νευρώνες. Η συνθήκη αυτή εξετάστηκε με το αν οι

αισθητήριους νευρώνες εξέφραζαν χαρακτηριστικούς δείκτες όπως ο TrkA, TrkB, TrkC.

Στην συνέχεια εξετάστηκαν και για δείκτες που ήταν πιο ειδικοί για ένα είδος αισθητήριου νευρώνα όπως το RunX1. Επιπρόσθετα, για να παρακολουθήσουμε την ανάπτυξη τους χρησιμοποιήσαμε δείκτες όπως στο PAX6, NESTIN, TUJ1, MAP2. Τέλος έγινε μελέτη για την έκφραση του Piezo2 που είναι ένας χαρακτηριστικός δείκτης που εκφράζεται στους μηχανοϋποδοχείς.

Table of Contents

ACKNOWLEDGEMENTS	1
ABSTRACT.....	3
ΠΕΡΙΛΗΨΗ.....	4
LIST OF TABLES	7
LIST OF FIGURES	7
CHAPTER 1.....	10
INTRODUCTION	10
1.1. GENERATION OF INDUCED PLURIPOTENT STEM CELLS (iPSCs).....	10
1.2. KEY PLURIPOTENCY TRANSCRIPTION FACTORS IN HESCs	11
1.3. MAJOR SIGNALLING PATHWAYS IN HESCs	13
1.3.1. FGF2.....	14
1.3.2. WNT.....	14
1.3.3. TGFβ/ACTIVIN/NODAL	15
1.3.4. MTOR: OVERVIEW	16
1.3.4.1. mTORC1	17
1.3.4.2. mTORC2	19
1.4. ASD AND SENSORY PROCESSING	20
1.5. TACTILE SENSORY DYSFUNCTION IN ASD.....	20
1.6. SENSORY NEURONS	21
1.7. BASIC PROTEINS DURING DIFFERENTIATION OF SENSORY NEURONS	22
1.7.1. BRN3A.....	22
1.7.2. RUNX.....	23
1.7.2.1. RUNX1.....	24
1.7.2.2. RUNX3.....	24
1.8. TACTILE SENSORY PHENOTYPES IN RODENT MODELS OF ASD ARE LINKED TO mTORC1.	24
CHAPTER 2.....	27
MATERIALS AND METHODS.....	27
2.1. CELL CULTURE AND CELL DIFFERENTIATION PROTOCOLS.....	27
2.1.1. NEURAL CREST AND SENSORY NEURON CULTURE CONDITIONS	28
2.1.2. IMMUNOPANNING PROTOCOL	29
2.1.3. CRYOSTORAGE OF SNS.....	30
2.2. BIOCHEMICAL METHODS.....	30
2.2.1. IMMUNOFLUORESCENCE ASSAY.....	30
2.2.2. FACS	31

2.2.3.	RNA EXTRACTION	31
2.2.4.	QUANTITATIVE REVERSE TRANSCRIPTION-POLYMERASE CHAIN REACTION (RT-QPCR)	32
CHAPTER 3		35
RESULTS		35
3.1.	EXPRESSION OF CHARACTERISTIC MARKERS OF SENSORY NEURONS	35
3.2.	EXPRESSION OF PIEZO2 TO XCL-1 DURING DIFFERENTIATION	42
CHAPTER 4		43
DISCUSSION		43
REFERENCES		47

List of Tables

Table 1: Protocol for the first step of qRT-PCR	33
Table 2: Protocol for the second step of qRT-PCR	33
Table 3: Table lists the name and sequence of primers used in this report, FW: Forward, RV: Reverse	34
Table 4: Table lists of antibodies. The name of the antibodies used in this report, accompanied by information regarding clone, species, company name, catalogue number and dilution factor.	Σφάλμα! Δεν έχει οριστεί σελιδοδείκτης.

List of Figures

Figure 1: Directed Differentiation of iPSCs	11
Figure 2: Dynamic transitions between pluripotent states in mice involve various methods.	13
Figure 3: Numerous kinase-driven signaling pathways regulate the key transcription factors associated with pluripotency, responding to both internal and external cues to uphold the self-renewal and differentiation capabilities of stem cells.	16
Figure 4: Function of mTORC1 and mTORC2 and their distinct roles in the cell.	17

Figure 5: Components and Architecture of human mTOR Complex 1.....	18
Figure 6: Components and Architecture of human mTOR complex 2.	19
Figure 7: Sensory pseudo-unipolar neurons in the dorsal root ganglion project one branch to the skin and another to the dorsal horn of the spinal cord.....	22
Figure 8: mTORC1 signalling regulates protein synthesis. Upstream and downstream signalling pathways.....	26
Figure 9: Protocol of differentiation	29
Figure 10: Images taken under optical microscope showing colonies of XCL-1 cells in mTeSRTM Plus medium and Vitronectin coated 6-well plates. Cells display a round shape and are tightly connected. 10x lens image.....	35
Figure 11: Images taken under optical microscope showing colonies of XCL-1 cells on day 2 of differentiation towards to sensory neurons. 4x and 20x lens image respectively.....	36
Figure 12: Expression of Pax6 and nestin on day 6 during the deafferentation of XCL-1 to sensory neurons	36
Figure 13: Image taken under optical microscope showing XCL-1 cells during differentiation. the cells start to have a star-like shape and had distanced themselves from the colonies. 4x and 10x lens image.....	37
Figure 14: Expression of tuja1 and RunX1 on day 10 of differentiation of XCL-1 cells towards to sensory neurons	37
Figure 15: Expression of TrkA, TrkB, TrkC on day 10 of differentiation of XCL-1 cells to sensory neurons	38
Figure 16: Images taken under optical microscope showing day 20 of differentiation for XCL-1 cells to sensory neurons. Cells had fully grown axons and dendrites. 10x and 20x lens image respectively	39
Figure 17: Expression of TrkA, TrkB, TrkC on day 20 of differentiation of XCL-1 cells to sensory neurons	39
Figure 18: Expression of tuja1 and RunX1 on day 20 of differentiation of XCL-1 cells towards to sensory neurons	40
Figure 19: Expression of TrkB and Map2 on day 20 of differentiation of XCL-1 cells towards to sensory neurons	40

Figure 20: Expression of TrkB and on day 65 of differentiation of XCL-1 cells towards to mechanosensory neurons	41
Figure 21: Images taken under optical microscope showing day 65 of differentiation for XCL-1 cells to sensory neurons. Cells had fully grown axons and dendrites. 20x lens image respectively	41
Figure 22: Expression of Piezo2 in different time point during the differentiation of XCL-1 cells to sensory neurons.	42

Chapter 1

Introduction

1.1. Generation of induced pluripotent stem cells (iPSCs)

Conventional embryology previously conceptualized embryonic development as a unidirectional pathway, positing that specialized cells inevitably forfeit their developmental potential. This perspective underwent a significant shift in 1962 when Gurdon's experiments with *Xenopus* challenged the notion of irreversible differentiation. In essence, Gurdon discovered that nuclei extracted from intestinal epithelial cells, when transplanted into an egg through somatic cell nuclear transfer (SCNT), could give rise to a fully developed tadpole, representing an entire organism (Hirai et al., 2011). The term "Nuclear Reprogramming" was subsequently coined to characterize the process that counteracts differentiation, returning a mature cell to its embryonic state (Hochedlinger & Jaenisch, 2006). Over several decades, researchers extensively investigated SCNT across various organisms (Mitalipov & Wolf, 2009). A pivotal breakthrough occurred in 1996 when scientists achieved the first successful generation of live sheep through the transplantation of nuclei from a cell line into a sheep oocyte (Campbell 1996, n.d.).

A decade after the initial strides in nuclear reprogramming, a groundbreaking advancement emerged. Researchers documented that mouse embryonic and adult fibroblasts could transform into cells resembling embryonic stem cells by introducing OCT4, SOX2, c-MYC, and KLF4. This remarkable achievement held the potential to pave the way for personalized regenerative therapy, addressing ethical concerns associated with human embryonic stem cells (hESCs) and circumventing issues related to donor-recipient compatibility (Takahashi & Yamanaka, 2006). In the subsequent year, two separate research groups achieved the creation of induced pluripotent stem cells (iPSCs) from human somatic cells. Yamanaka's team reprogrammed adult human fibroblasts using the same transcription factors proven successful in mice (Takahashi et al., 2007). Meanwhile, Thomson's group retained OCT4 and SOX2 but substituted the other two factors with NANOG and LIN28 (J. Yu et al., n.d.).

However, shortly after the discovery of induced pluripotent stem cells (iPSCs), researchers expressed concerns regarding their resemblance to human embryonic

stem cells (hESCs) and their safety. In 2013, a comprehensive study compared 49 iPSC lines with 10 hESC lines, analyzing mRNA expression and DNA methylation, and identified no significant differences. Nevertheless, the study highlighted that certain iPSC lines exhibit resistance to neuronal differentiation, leading to tumor formation upon transplantation in mice (Koyanagi-Aoi et al., 2013). The Human Induced Pluripotent Stem Cell Initiative, which generated 711 iPSC lines from 301 healthy donors, aimed to elucidate the reasons behind the observed heterogeneity in iPSC lines. Their findings indicated that a substantial portion of the variations is attributable to the diverse donor origins of the cells (Kilpinen et al., 2017).

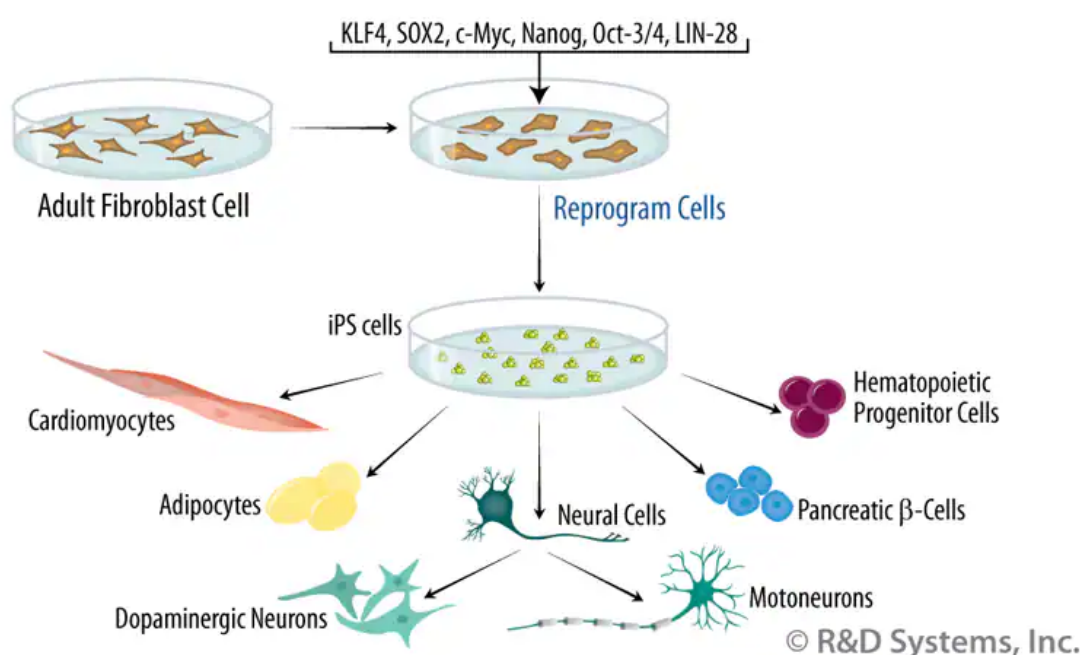


Figure 1: Directed Differentiation of iPSCs. Induced pluripotent stem cells (iPSCs) are generated by reprogramming adult somatic cells. Following isolation, somatic cells are cultured *in vitro* and transduced with expression vectors encoding transcription factors associated with pluripotency. For most cell types, four factors (c-Myc, Oct-3/4, SOX2, and KLF4) are used, although a combination of alternate factors (Oct-3/4, SOX2, Nanog, and LIN-28) has also been used successfully. Adapted from: (J. Yu et al., n.d.)

1.2. Key pluripotency transcription factors in hESCs

Numerous transcription factors play a crucial role in maintaining the pluripotency of mouse embryonic stem cells (mESCs) (Loh & Lim, 2011). Among these, NANOG, OCT4, and SOX2 are considered the core components of pluripotency (Silva & Smith, 2008). The gene *Pou5f1* encodes OCT4, also known by alternative names such as OCT3, OCT3,4, OTF3, and NF-A3 (Zeineddine et al., 2014). OCT4 is a member of a protein family that binds to the octamer motif ATGCAAAT and is present in unfertilized oocytes,

ESCs, and Primordial Germ Cells (PGCs) (Scholer et al., 1989). Disturbing OCT4 levels in mESCs leads to differentiation, where the absence of OCT4 results in trophectoderm (TE) cell formation, while an increase in OCT4 expression leads to the activation of mesodermal and endodermal markers (Niwa et al., 2000).

Leukemia inhibitory factor (LIF) plays a role in maintaining mESCs in an undifferentiated state (Williams et al., 1988), and the central transcription factor downstream of LIF is STAT3 (Niwa et al., 1998). NANOG, a homeoprotein, independently sustains pluripotency in mESCs irrespective of LIF (Chambers et al., 2006.) . Simultaneously, NANOG is not essential for self-renewal. Additionally, NANOG levels exhibit variability in mESCs, a phenomenon explained by the rheostat model. This model suggests that mESCs can reversibly transition from a state of high NANOG expression to a low NANOG state. The latter state is permissive for differentiation as long as external stimuli direct fate acquisition; otherwise, mESCs return to their normal pluripotent state (Chambers et al., 2007).

SOX2 is a member of the SOX (Sry-related HMG box) protein family, known for its ability to bind to DNA through the HMG domain (Kamachi, 2000). Mice lacking SOX2 due to mutations can form blastocysts, but they face post-implantation mortality. In cultured mutant blastocysts, improper specification of the inner cell mass (ICM) occurs, leading to the development of trophectoderm (TE) and primitive endoderm (PE). The presence of maternal SOX2 in the ICM suggests a potentially crucial role for SOX2 in earlier developmental stages (Avilion et al., 2003) . To fully understand the developmental significance of this transcription factor, further investigations targeting both maternal and embryonic SOX2 are necessary. Such studies would provide insights into the similarity between the SOX2 mutant phenotype and the OCT4 mutant phenotype (Chambers & Smith, 2004).

SOX2 plays a vital role in maintaining pluripotency in mouse embryonic stem cells (mESCs), as evidenced by the differentiation of SOX2-null mESCs into TE cells. This phenotype aligns with the observed differentiation of OCT4-null mESCs. Additionally, SOX2 appears to influence pluripotency by regulating the expression of OCT4. In the absence of SOX2, ES cells upregulate the expression of negative regulators of OCT4, such as Nr2f2, while downregulating positive regulators like Nr5a2 and OCT4 itself (Masui et al., 2007).

NANOG, OCT4, and SOX2 collaboratively participate in the transcriptional regulation of human embryonic stem cells (hESCs), evidenced by significant overlap in their target genes and concurrent binding to the genes encoding these factors (Boyer et al., 2005) . Despite their role in pluripotency, these key factors are also implicated in differentiation. Each factor favors the acquisition of distinct cell fates. Elevated OCT4 levels contribute to self-renewal, while low levels are incompatible with pluripotency. OCT4 knockdown hESCs undergo embryonic ectoderm differentiation in the absence of stimulation but exhibit extraembryonic differentiation upon BMP4 induction . Furthermore, NANOG inhibits the formation of neuroectoderm (NE) and neural crest, while SOX2 inhibits mesendoderm (ME) differentiation (Wang et al., 2012) . These findings underscore the versatile utilization of the same molecular machinery in development to achieve diverse goals based on the needs of the developing organism.

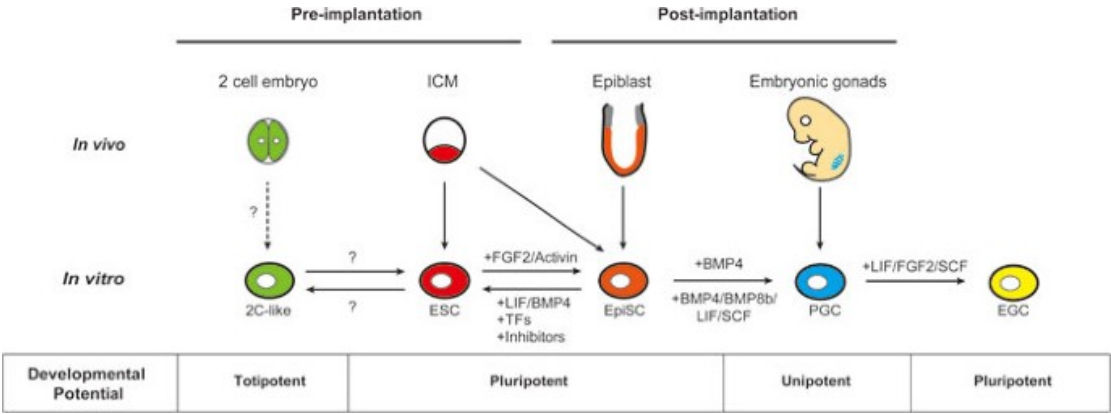


Figure 2: Dynamic transitions between pluripotent states in mice involve various methods. Mouse embryonic stem cells (mESCs) originate from the inner cell mass (ICM) of pre-implantation blastocysts, while epiblast stem cells (EpiSCs) are derived from the post-implantation embryo's epiblast compartment. Conversion between the pluripotent mESC and EpiSC states is achievable through cell culture, the introduction of transcription factors (TFs), or the use of chemical inhibitors. Unipotent primordial germ cells (PGCs) are derived from the embryonic gonad and can be differentiated from EpiSCs using BMP4 alone or in combination with BMP8b, leukemia inhibitory factor (LIF), and stem cell factor (SCF). Subsequently, PGCs can be reprogrammed to pluripotency through culture with LIF, fibroblast growth factor 2 (FGF2), and SCF, resulting in the formation of mouse embryonic germ cells (EGCs). Additionally, mESCs have the ability to transiently transition into a 2-cell (2C)-like state with expanded developmental potential, generating both embryonic and extraembryonic tissues. However, the process and mechanism of this 2C transition remain unknown, and whether 2C-like cells can be directly isolated from 2C embryos has not been established. (CITATION: The transcriptional regulation of pluripotency)

1.3. Major Signalling Pathways in hESCs

Numerous signaling pathways play a crucial role, either directly or indirectly, in maintaining the pluripotent state and regulating the differentiation of stem cells. The following section will delve into the most significant of these pathways.

Despite sharing a common origin and similarities in self-renewal and pluripotency, mouse embryonic stem cells (mESCs) and human embryonic stem cells (hESCs) exhibit differences. In mESCs, properties are influenced by the LIF and BMP (Bone Morphogenetic Proteins) signaling pathways, while in hESCs, these pathways are not effective. Instead, hESCs rely on Activin and FGF for their pluripotency properties.

1.3.1. FGF2

Regarding Fibroblast Growth Factor 2 (FGF2), this protein family serves as a key regulator in various fundamental processes, including survival, proliferation, migration, differentiation, embryonic development, organogenesis, tissue repair, and metabolism. The FGF family encompasses twenty-two members and four specific transmembrane tyrosine kinase receptors. Ligand binding to an FGF receptor (FGFR), stabilized in the presence of heparin or heparin sulfate, activates an intrinsic receptor tyrosine kinase, leading to autophosphorylation (Dailey et al., 2005) .

In human ESCs, the activation of FGFRs triggers signal transduction through two additional pathways: PI3K-AKT and MEK-ERK. Activation of either the PI3K or AKT pathway has distinct effects on pluripotency. AKT activation, through mTOR signaling, inhibits apoptosis, enhances cell proliferation, and simultaneously inhibits ERK signaling, responsible for hESC differentiation. Conversely, PI3K activation is crucial for initiating the differentiation process in hESCs. These observations suggest that FGF signaling effectively operates via PI3K/AKT in maintaining hESCs pluripotency, while the MAPK signaling pathway is essential for pluripotent hESCs (Li et al., 2007) .

FGF2 plays a multifaceted role in maintaining hESCs pluripotency, with exogenous recombinant hFGF2 supplementation in hESC culture media primarily contributing to pluripotency maintenance by promoting cell adhesion and survival.

1.3.2. Wnt

Wnt ligands, part of the extensive Wnt protein family, play a pivotal role in influencing cell proliferation, establishing cell polarity, determining cell fate in embryonic development, and regulating the delicate balance between self-renewal and

differentiation (Logan & Nusse, 2004) . The action of Wnt proteins involves multiple Frizzled receptors and LRP5/6 coreceptors. Binding of Wnt ligands to these receptors stabilizes cytosolic β -catenin by recruiting Axin to the membrane, leading to the phosphorylation of LRP and subsequent inhibition of glycogen synthase kinase-3 (GSK-3)-dependent phosphorylation of β -catenin. Consequently, β -catenin translocates to the nucleus and activates Wnt target genes. Simultaneously, the inhibition of GSK-3 activates the mTORC1 kinase, a master regulator of growth, proliferation, and mRNA translation. The Wnt activation pathway also sustains the expression of pluripotency factors such as Nanog, Sox2, and Oct4. In the absence of Wnt, β -catenin is targeted by the proteasome complex consisting of the scaffold Axin, casein kinase-1 (CK1), GSK-3, and adenomatous polyposis coli (APC), leading to its degradation (Bhavanasi & Klein, 2016).

1.3.3. TGF β /Activin/Nodal

The TGF- β superfamily encompasses a diverse array of proteins, including TGF- β , activin, nodal, inhibin, lefty, and bone morphogenetic proteins (BMPs). Within this superfamily, three classes of receptors have been identified: type I (TGFRI or activin-like kinases ALKs), type II (TGFRII), and type III (TGFRIII). Upon binding of TGF- β family proteins to these receptors, receptor activation occurs, followed by interaction with Smad family proteins. These Smad proteins undergo phosphorylation in the cytoplasm and are then translocated to the nucleus, where they act as transcriptional cofactors to activate target genes that determine cell fate.

Certain members of the TGF- β superfamily are enriched in stem cells and play crucial roles in self-renewal, maintenance of pluripotency, and differentiation (Park, 2011). Studies in mice have demonstrated that Nodal-deficient embryos exhibit an epiblast with significantly reduced Oct4 expression, suggesting that Nodal signals contribute to the preservation of embryonic stem cell (ESC) identity (Robertson et al., 2003). Research has also indicated that Activin/Nodal signaling plays a significant role in maintaining pluripotency in human ESCs by controlling NANOG expression, thereby preventing neuroectoderm differentiation of pluripotent cells (Vallier et al., 2009). Additionally, NANOG expression is induced by TGF- β /activin-mediated SMADs, which

bind directly to their receptor, and by activin, which also induces OCT4 expression (Xiao et al. ,2006).

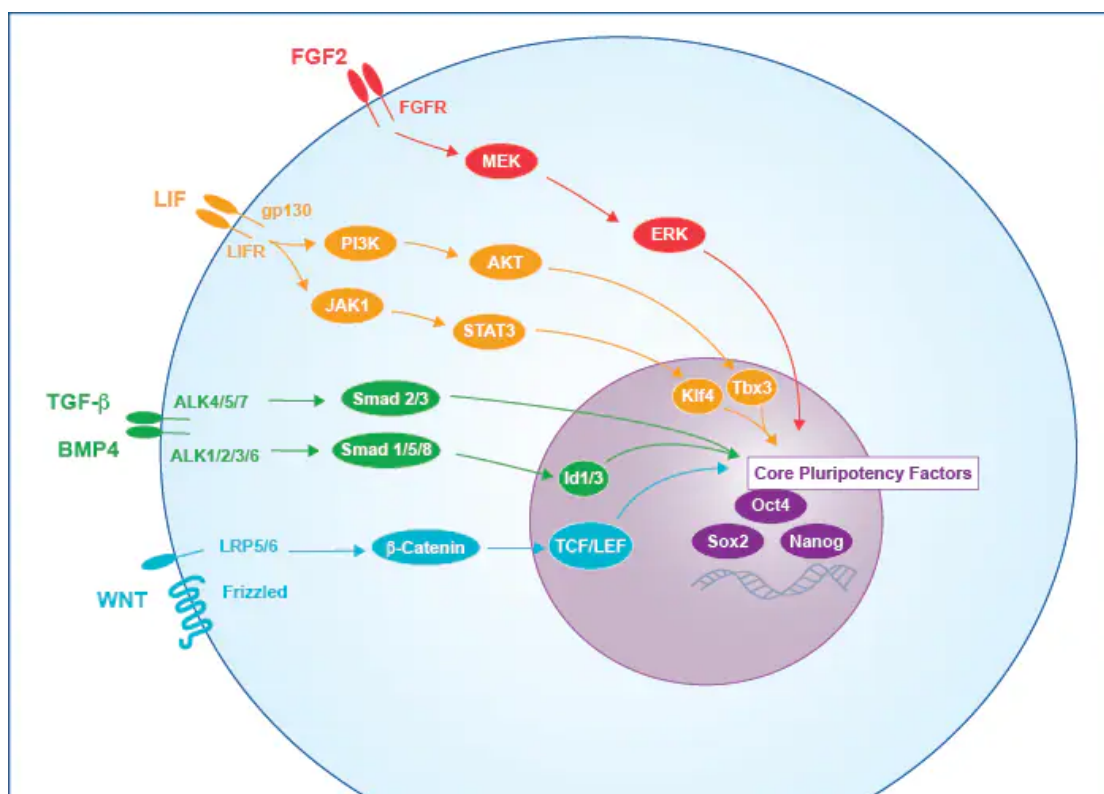


Figure 3: Numerous kinase-driven signaling pathways regulate the key transcription factors associated with pluripotency, responding to both internal and external cues to uphold the self-renewal and differentiation capabilities of stem cells. The collaborative action of these pathways synergistically ensures the preservation of pluripotency.

1.3.4. mTOR: Overview

Mammalian target of rapamycin (mTOR) is a serine/threonine protein kinase that was initially identified as the cellular target of rapamycin. In 1964, a team of researchers was able to isolate from a *Streptomyces hygroscopicus* soil bacterium, a novel macrolide with potent antifungal activity and immunosuppressive, anti-tumor and neuroprotective properties as later demonstrated. The macrolide was named rapamycin after its place of origin, the island Rapa Nui (Easter Island) (Vezina et al., n.d.) . In 1990, rapamycin was shown to act in part by binding the prolyl-isomerase FKBP12, thus forming a gain-of-function complex that broadly inhibits cell growth and proliferation (Chung et al. ,1992) . The full mechanism of action was elucidated four years later, in 1994, when a large kinase was identified through experiments, which

acts as the mechanistic (originally 'mammalian') target of rapamycin (mTOR) in mammals.

mTOR is a 289-kDa serine/threonine protein kinase and belongs to the phosphatidylinositol 3-kinase (PI3K)-related kinase (PIKK) family. mTOR interacts with other subunits to form two distinct complexes known as mTOR complex 1 (mTORC1) and mTORC2. These two complexes are distinguished by their accessory proteins, their differential sensitivity to rapamycin, their unique substrates and functions and as well by their signalling roles in the cell (Liu & Sabatini, 2020)

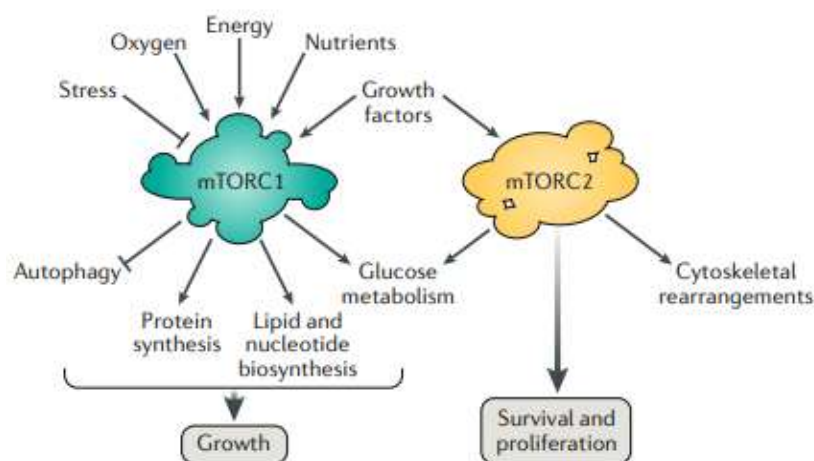


Figure 4: Function of mTORC1 and mTORC2 and their distinct roles in the cell. mTORC1 integrates information about nutritional abundance and environmental status including growth factors, amino acids, and stress to tune the balance of anabolism and catabolism in the cell, so it coordinates cell growth. mTORC2 governs cell survival by activating several pro-survival pathways, cytoskeletal behavior, and migration through phosphorylating glucocorticoid-regulated kinase (SGK), protein kinase B (AKT), and protein kinase C (PKC) kinase families. mTORC1, which is acutely inhibited by rapamycin, mTORC2 responds only to chronic rapamycin treatment. Source:(Liu & Sabatini 2020)

1.3.4.1. mTORC1

mTORC1 is assembled by three core components: mTOR, mammalian lethal with protein regulator-associated protein of mTOR (RAPTOR). RAPTOR coordinates the appropriate subcellular localization of mTORC1, while it recruits mTORC1 substrates through TOR signalling motifs, which are present on several canonical mTOR substrates. Additionally, a scaffold is formed by RAPTOR for the mTORC1 accessory factor proline rich AKT substrate 40kDa (PRAS40), which as an endogenous inhibitor of

mTORC1 activity alongside DEP-domain-containing mTOR-interacting protein (DEPTOR) (Peterson et al., 2009). mTORC1 is associated with a number of cellular processes, including repression of autophagy, synthesis of proteins and lipids, lysosome biogenesis and growth factors signalling.

The activation of mTORC1 leads to the phosphorylation of PRAS40, the complex's negative regulator, decreasing mTORC1-PRAS40 binding and enhancing mTORC1 signalling. mTOR is capable to controlling its own activation by DEPTOR's degradation, the second negative regulator. mTORC1 substrates are recruited by RAPTOR, such as ribosomal S6 kinase (S6K) and eIF4E-binding protein (4EBP1). mTORC1 controls protein synthesis through phosphorylation of S6K and 4EBP1 and lipid synthesis through STEROL-responsive element binding protein (SREBP) transcription factors, which can be activated by S6K or the phosphatidate phosphatase lipin 1 (Peterson et al., 2011). Meanwhile, the process of autophagy is controlled by mTORC1 for instance when nutrients are abundant, Unc-51-like kinase 1 (ULK1) is phosphorylated, blocking ULK1 activation by 5' adenosine monophosphate- activated protein kinase (AMPK) and preventing autophagy (Kim et al., 2013). Lastly, PI3K and mitogen-activated protein kinase (MAPK)-mediated growth factor signalling is negatively regulated by mTORC1, via phosphorylation and stabilization of growth factor receptor-bound protein 10 (Grb10) (Y. Yu et al., 2011).

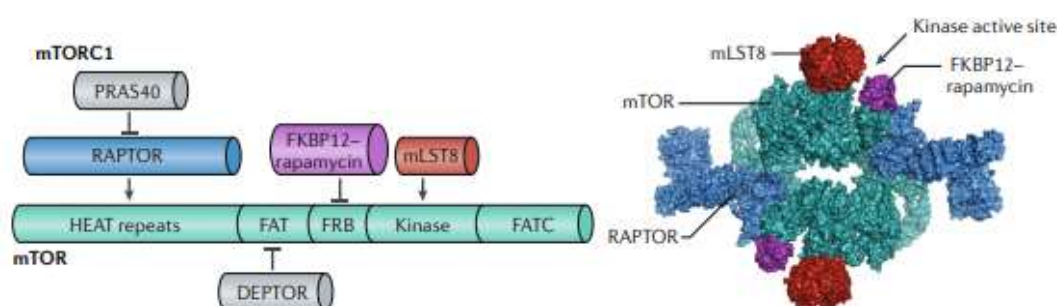


Figure 5: Components and Architecture of human mTOR Complex 1. mTOR is constituted by HEAT repeats (Clusters of huntingtin, elongation factor 3, proteins phosphatase 2A and TOR1), FAT (FRAP, ATM and TRRAP), FRB (the FKBP12–rapamycin binding) and FATC domain, which constitute a binding site region for the other mTORC1 subunits. Via this HEAT repeats domain, RAPTOR is bound to mTOR, and it is required for lysosomal localization of the complex. PRAS40 is recruited by RAPTOR and inhibits the mTOR activity. DEPTOR is bound at the FAT domain and it is an endogenous inhibitor of mTORC1 activity. FRB domain is inhibited by FKBP12–rapamycin and mammalian lethal with SEC13 protein 8 (mLST8) is bound at the catalytic kinase domain of mTOR. Adapted from: (Liu & Sabatini 2020).

1.3.4.2. mTORC2

The core of mTORC2 is formed by mTOR and mLST8, which is requisite for the stability and function of mTORC2, and its defining subunit, the unrelated scaffolding protein RICTOR (Hwang et al., 2019). MAPK-interacting protein 1 (mSIN1) and protein associated with Rictor 1 or 2 (PROTOR1/2) are attracted and bound by the RICTOR, and they coordinate to nucleate the complex. mSIN1 has a phospholipid-binding pleckstrin homology domain which is claimed to help mTORC2 assemble on the plasma membrane (Yuan & Guan, 2015). Also, studies have shown that knockdown of RICTOR, mTOR or mLST8 but not RAPTOR prevents the reorganization of actin cytoskeleton network, while inhibiting chemotaxis and migration (Jacinto et al., 2004). mTORC2 is connected to cell survival, cell growth and proliferation, and cytoskeletal remodeling (Unni & Arteaga, 2019). mTORC2 phosphorylates several kinases including protein kinase C (PKC α , δ , ζ , γ , ϵ), RAC- α serine/threonine protein kinase (AKT/PKB) and serum/glucocorticoid-regulated kinase 1 (SGK1). PKC phosphorylation is associated with the regulation of cytoskeletal remodeling and cell migration, AKT promotes cell growth and proliferation while SGK1 controls ion transport and cell survival.

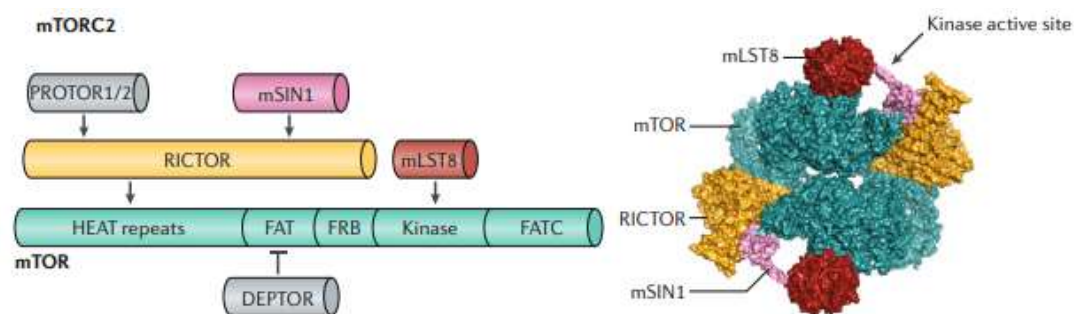


Figure 6: Components and Architecture of human mTOR complex 2. As in mTORC1, mTOR structure does not change, HEAT repeats, FAT, FRB, Kinase and FATC domains. mTORC2 is defined of RICTOR, which is bound to mTOR via HEAT repeats and recruits RICTOR1/2 and mSIN1 to the complex. mLST8 is bound to kinase domain. In lieu of mTORC1, FKBP12-rapamycin is not united at mTOR, in contrast to mTORC1, in mTORC2 FKBP12-rapamycin is not bound to mTOR. The binding is inhibited by RICTOR, rendering mTORC2 insensitive to acute inhibition by rapamycin. Source: (Liu and Sabatini 2020)

1.4. ASD and Sensory Processing

Autism Spectrum Disorder (ASD) is a prevalent neurodevelopmental disorder characterized by social deficits and stereotyped repetitive behaviours. Approximately 95% of individuals with ASD exhibit sensory abnormalities, with ~60% displaying altered tactile sensitivity¹. Sensory processing abnormalities in ASD manifest in hypersensitivity, avoidance of sensory stimuli, diminished responses to sensory stimulation, and/or sensory seeking behaviour, depending on the context (Baranek et al., 2006; Iarocci & McDonald, 2006). The sensory domain arguably holds great promise for revealing mechanisms central to the pathogenesis of ASD. Sensory abnormalities in ASD are amongst the most replicable features of these disorders (Ben-Sasson et al., 2008; Klintwall et al., 2011), present in early childhood (Elison et al., n.d.; Klintwall et al., 2011) and are strong predictors of behavioural symptoms manifesting later in life (Green et al., 2012; Sullivan et al., 2014). Not surprisingly, sensory processing difficulties constitute an ASD diagnostic criterion in the Diagnostic and Statistical Manual of Mental Disorders, 5th edition (DSM-5).

1.5. Tactile Sensory Dysfunction in ASD

To explore our environment and for sensorimotor control, we require the sense of touch. Moreover, across many species, social touch and formation of relationships rely upon tactile sensation. During development, gentle touch communication between mother and infant is essential for cognitive, motor, and social processes. The spinal cord serves as the relay station between the skin and brain, and is the first location where the body prioritizes how much touch versus pain information reaches the brain and our conscious awareness (Sullivan et al., 2014). Despite the heterogeneity of ASD cohorts and the diversity of tactile sensitivity measures, tactile processing dysfunctions have been reported in several clinical (Rogers et al., 2003) and psychophysical (Tavassoli et al., 2014) studies of ASD patients (Kojovic et al., 2019). These studies suggest that tactile processing abnormalities detected in children persist into adulthood and may have a link to core autism phenotypes (social, repetitive behaviours). For example, hypersensitivity of peripheral neurons may contribute to avoidance of social touch, a common behavioural phenotype in individuals with ASD.

Hyposensitivity in the peripheral nervous system may result in an inadequate amount of touch information reaching the brain, causing individuals to be indifferent to social touch.

1.6. Sensory neurons

The neural crest, a dynamic cell group in vertebrate development, is integral to the creation of diverse cell types. Neural crest cells (NCCs), emerging from the neural tube, undergo delamination and migrate under strict spatiotemporal control by neural tube signals. Notably, some NCCs migrate ventrally, navigating between the dermamyotome and neural tube to form the dorsal root ganglia (DRG). This process illustrates the orchestrated development of various cell types, emphasizing the neural crest's role as a model system for investigating the intricacies of neuronal diversity establishment.

The dorsal root ganglia (DRG) neurons exhibit a remarkable diversity, each type specialized for distinct perceptual modalities. These neurons are characterized by unique molecular features, including the presence or absence of neuropeptides, such as neurotrophic tyrosine receptor kinase A-containing (TrkA+) peptidergic neurons and TrkA– non-peptidergic neurons. Additionally, they possess specific sets of ion channels that contribute to their ability to respond to particular stimuli.

The response patterns of DRG neurons are varied: small-diameter neurons with thinly myelinated or unmyelinated axons, encompassing TrkA+ peptidergic and TrkA– non-peptidergic neurons, are often associated with noxious stimuli and play a role in mediating pain sensations (nociceptive neurons). On the other hand, larger-diameter neurons, including TrkB+ and/or TrkC+ subtypes, specialize in conveying mechanical sensations, such as touch. Furthermore, large proprioceptive neurons, particularly TrkC+ neurons, are instrumental in sensing limb movement and position.

In essence, the distinctive characteristics of DRG neurons, from molecular composition to responsiveness, underscore their specialization in diverse sensory functions, encompassing nociception, mechanoreception, and proprioception.

In the initial stage of somatosensory perception, the activation of primary sensory neurons is essential, and these neurons have their cell bodies located within dorsal root ganglia (DRG) and cranial sensory ganglia. The structure of DRG neurons is pseudo-unipolar, featuring one axonal branch extending to the periphery to connect with peripheral targets. Simultaneously, another branch penetrates the spinal cord, forming synapses onto second-order neurons in the spinal cord gray matter and, in certain cases, the dorsal column nuclei of the brainstem. As a result, the majority of DRG neurons exhibit heightened sensitivity to nociceptive and thermal stimuli.

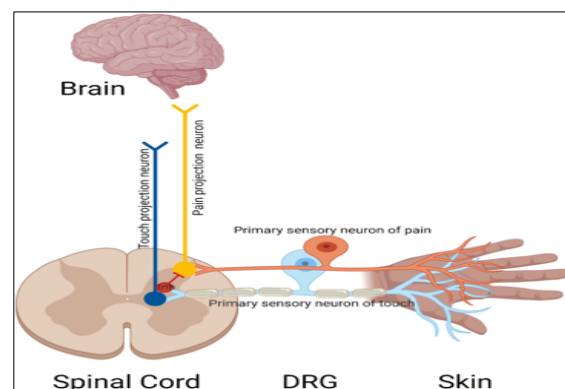


Figure 7: Sensory pseudo-unipolar neurons in the dorsal root ganglion project one branch to the skin and another to the dorsal horn of the spinal cord. Distinct subtypes of primary sensory neurons detect noxious and innocuous stimuli. These cells activate second order neurons in the spinal cord (interneurons or projection neurons) which deliver somatosensory information to the brain. Adapted from ref.¹⁷; DRG: Dorsal Root Ganglia..

The distinction between innocuous and noxious tactile sensations is dependent on specialized mechanosensitive sensory neurons falling into two main categories: low-threshold mechanoreceptors (LTMRs) responsive to innocuous mechanical stimuli and high-threshold mechanoreceptors (HTMRs) activated by potentially harmful mechanical stimuli.

1.7. Basic proteins during differentiation of Sensory Neurons

1.7.1. BRN3A

Beginning just prior to cell cycle exit, nearly all embryonic sensory neurons co-express the POU-homeo- domain transcription factor Brn3a and (Fedtsova et al., 2003) . Sensory neurons lacking these factors exhibit multiple defects in sensory axon growth, and die in the perinatal period (Xiang et al., 1996). In the DRG and TG, Brn3a facilitates the progression of sensory development by terminating the expression of neurogenic bHLH factors by direct repression , defining one common function for these pan-sensory factors. Brn3a creates a permissive condition for subtype specification by promoting Runx1 and Runx3 expression, which then refine sensory neuron phenotypes by repressing TrkB in prospective TrkA- and TrkC-expressing neurons,

respectively. Although Brn3a binds directly to a Runx3 enhancer element, it is clear that this is a necessary but not sufficient condition for the initiation of Runx3 expression since Brn3a is widely expressed at the onset of Runx3 expression, yet Runx3 is only initiated in a subset of Brn3a neurons.(Raisa Eng et al., 2007)

Beginning just before exiting the cell cycle, nearly all sensory neurons during embryonic development express the Brn3a transcription factor. Deficiencies in sensory axon growth and perinatal death are observed in sensory neurons lacking Brn3a. In the dorsal root ganglia (DRG) and trigeminal ganglia (TG), Brn3a plays a vital role in promoting sensory development by directly repressing the expression of neurogenic basic helix-loop-helix (bHLH) factors, indicating a shared function among these pan-sensory factors(Raisa Eng et al., 2007) .

Brn3a establishes a permissive environment for subtype specification by encouraging the expression of Runx1 and Runx3. This, in turn, refines sensory neuron phenotypes by suppressing TrkB in potential TrkA- and TrkC-expressing neurons. Despite Brn3a directly interacting with a Runx3 enhancer element, it is apparent that this interaction is necessary but not sufficient for the initiation of Runx3 expression. This is underscored by the fact that although Brn3a is broadly expressed at the onset of Runx3 expression, Runx3 is only initiated in a specific subset of Brn3a-positive neurons.

1.7.2. RUNX

The RUNX family of transcription factors have key roles in the diversification of sensory neurons (Marmigère et al., 2006) . Preliminary findings indicate that two of the three members, *Runx1* and *Runx3*, are differentially expressed in DRG sensory neurons in a non-redundant manner such that RUNX1 is found in small TrkA+ neurons and RUNX3 in large TrkC+ neurons (Levanon et al., n.d.) . Blocking both RUNX1 and RUNX3 activities in the chick results in a loss of TrkA+, TrkB+ and TrkC+ neurons. The RUNX family of transcription factors plays crucial roles in the differentiation of sensory neurons. Initial observations suggest that among the three members, namely Runx1 and Runx3, their expression in DRG sensory neurons is distinct and non-redundant. Specifically, RUNX1 is identified in small TrkA+ neurons, while RUNX3 is prevalent in

large TrkC⁺ neurons. Inhibition of both RUNX1 and RUNX3 functions in chick models leads to the depletion of TrkA⁺, TrkB⁺, and TrkC⁺ neurons.

1.7.2.1. RUNX1

Runx1 is expressed specifically in an early TrkA⁺ population during embryogenesis (Theriault et al., 2004) whereas postnatally its expression becomes more restricted to a subtype of nociceptors arising from the TrkA⁺ population. RUNX1 is also involved in the further diversification of the TrkA⁺ neurons into different types of nociceptors during late embryonic and postnatal stages (Chen et al., 2006). At these points, RUNX1 seems to act as a repressor. All embryonic small neurons initially express *TrkA*. During postnatal development, some nociceptors stop expressing *TrkA* and begin to express *Ret*.

1.7.2.2. RUNX3

RUNX3 is first detected in DRG and cranial ganglia, it is confined to all TrkC⁺ neurons. RUNX3 might also be important at later embryonic stages. It seems to participate in the diversification into different subclasses of the early TrkC⁺ population produced during the first and second waves of neurogenesis, including the TrkC⁺ proprioceptors and several TrkB/TrkC neuronal subtypes. Two distinct and transient populations of *TrkB/TrkC* and *TrkB/Ret*-expressing DRG neurons exist at early stages. (Levanon D, 2002)

1.8. Tactile Sensory Phenotypes in rodent models of ASD are linked to mTORC1.

ASD is a polygenic disorder and though the prevalence of syndromic autism is not high (~15%), studying the effects of single mutations facilitates the elucidation of the polygenic aetiology. In several monogenic disorders, which are co-diagnosed with high rates of autism such as fragile X syndrome (*Fmr1*), Rett syndrome (*Mecp2*) and Phelan-McDermid Syndrome there is a hyperactivation of a key kinase in the brain, mTORC1 (mechanistic target of rapamycin). The best-studied and understood function of

mTORC1 is the control of mRNA translation and the majority of regulation is exerted at the level of initiation. Ribosome recruitment to the mRNA requires a group of translation initiation factors, termed eIF4 (eukaryotic initiation factor 4). A critical member of this group is eIF4F (Grifo et al., 1983). eIF4E a key subunit of eIF4F, interacts with the 5' mRNA cap structure (m⁷GpppN, where N is any nucleotide) (Sonenberg et al., 1979). Although eIF4F complex assembly is regulated via several modes, the best-characterized mechanism involves the members of a family of three small molecular weight proteins, the eIF4E-binding proteins (4E-BPs). Non-phosphorylated 4E-BPs bind with high affinity to eIF4E, thus preventing eIF4F complex formation and consequently inhibit translation (Gingras et al., 1999). Upon phosphorylation by mTORC1, 4E-BPs dissociate from eIF4E, allowing eIF4F complex formation and relief of translation inhibition. 4E-BPs have been implicated recently in ASD (Gkogkas et al., 2013). eIF4F in various systems regulates translation of a subset of mRNAs, rather than equal, across the board increase in global translation (Hay & Sonenberg, 2004). Interestingly, recent work has demonstrated that cellular abundance of proteins (~54% of the protein concentration) is predominantly established at the level of translation (Schwanh usser et al., 2011). Fragile X syndrome (FXS), Rett syndrome and Phelan-McDermid Syndrome patients display tactile hypersensitivity. *FMR1* and *SHANK3* mutations account for ~5% of syndromic ASD cases (Moessner et al., 2007; Wassink et al., n.d.). Rett Syndrome (*MECP2*) is a debilitating neurodevelopmental disorder affecting 1 in 10,000 individuals. FXS is the most common known cause of inherited intellectual disability and is caused by CGG expansions in the *Fmr1* gene promoter leading to loss of function (Hagerman et al., 2017). *Fmr1* is an inhibitor of protein synthesis and its loss of function engenders hyperexcitability, synaptic dysfunction (exaggerated metabotropic glutamate receptor long-term depression; mGluR-LTD) and exaggerated protein synthesis, affecting specific mRNAs identified in previous studies (~800 mRNAs including autism risk genes and several genes expressed in sensory neurons) (Darnell et al., 2011). Strikingly, *Fmr1*, *Mecp2* and *Shank3* knockout (KO) mice displayed altered tactile discrimination and hypersensitivity to gentle touch, accompanied by sensory neuron hyperexcitability, along with core behavioural deficits reminiscent of ASD (social, cognitive, and repetitive/stereotypic) (L. L. Orefice et al., 2019; L. L. L. Orefice et al.,

2016) . Collaborative work from the Gkogkas lab revealed that 4E-BP1 deletion in mice leads to mechanical, but not thermal hypersensitivity (Khoutorsky et al., 2015a) , suggesting that the mTORC1/4E-BP1 axis is critical for tactile sensation. Furthermore, a subset of mRNAs is translationally controlled in mechanosensory cells downstream of mTORC1/4E-BP1. (Wong et al., 2023)

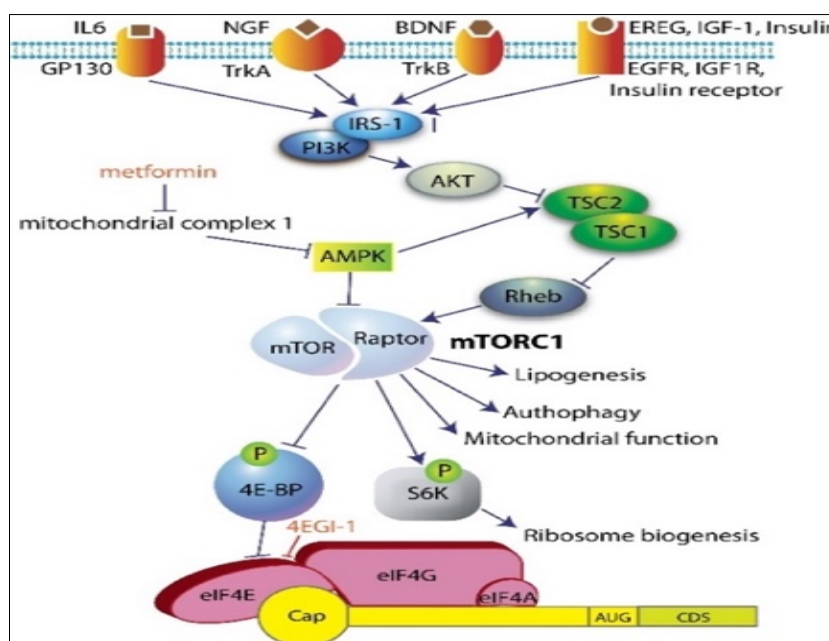


Figure 8: mTORC1 signalling regulates protein synthesis. Upstream and downstream signalling pathways

The mechanisms going awry in familial forms of ASD (e.g. Fragile X Syndrome) may also be implicated in sporadic forms of ASD, given the pervasive role of the mTORC1/4E-BP1 signalling pathway in regulation of cellular functions. On the other hand, sensory abnormalities are common in rodent models of ASD. There is growing evidence that sensory hypersensitivity, especially tactile hypersensitivity, may contribute to social deficits and other autism-related behaviors. For all these reasons:

Thesis Aim: To develop a chemical differentiation protocol from human iPSCs cells into sensory neurons, focusing on mechanosensory neurons. This model will be used to study the potential link between mTORC1/4E-BP1-dependent translational control and tactile hypersensitivity in neurodevelopmental disorders.

Chapter 2

Materials and Methods

2.1. Cell culture and Cell Differentiation Protocols

Human induced pluripotent stem cells (hiPSCs) must be handled carefully and fed certain nutrients to preserve their pluripotency throughout maintenance. The medium utilized for this purpose was Essential 8™ Medium (Thermo Scientific A1517001), an animal serum free, completely chemically defined nutrition and xenobiotic agent. It is based on the E8 formulation developed by the laboratory of Dr. James Thomson (University of Wisconsin-Madison).

All experiments were performed using iPSCs XL1 cell line. Six-well tissue culture plates (SPL, cat. 30006) were coated with 80µl vitronectin diluted in 8ml DMEM/F12 (Hyclone, cat. SH30023.01) medium (Dilution factor 1:100), and incubated for 1h at room temperature. The vitronectin solution was then removed, wells washed x 1 with DMEM/F12 and cells plated into the well. Spontaneously differentiating cells were manually removed from the cultures. The percentage of these cells was always less than 10% and is an indicator of a healthy culture. Only cultures meeting this criterion were used in the experiments.

The iPSCs were passaged when most colonies were ~1 mm in diameter and can be seen with naked eye. Once visible colonies appear, compact with dense centers and their borders were beginning to fuse passage the iPSC colonies with EDTA (Invitrogen, cat. AM9260G). Cells were washed with 1ml of DMEM/F12 and passaged enzymatically using 1ml of 0.5mM EDTA in PBS for 5min at 37°C until the edges of the colonies started to shrink but without the colonies detaching from the dish. At the end of the incubation, the EDTA was removed and 2 washes of the well with 2ml DMEM/F12 were performed to remove all enzyme residues. To harvest the hESCs colonies, 1ml of E8 medium was added and using a scraper the colonies were detached from the surface of the dish and transferred to a 15ml falcon tube with a 5ml pipette. To be sure that all cells were transferred, and that no selection for less adherent

colonies occurred, this procedure was performed twice or thrice. Namely, another 1ml of E8 medium was added to the well and using a scraper, all remaining cells were scraped off and transferred to the falcon tube. The fragmented iPSC colonies were then dissociated into small clumps by gentle agitation to obtain the appropriate size required and replated onto vitronectin-coated six well plates in a 1:10 ratio. Finally, the dish was very gently shaken and placed in the 37°C incubator with 5% CO₂ for 4–6 days; the medium was changed every day until the iPSC colonies are ~1mm in diameter and are visible with the naked eye.

Prior to freezing, iPSCs cells were passaged from 6-well plates as described above and collected in 15mL falcon tubes. They were centrifuged at 1000rpm for 5min at room temperature and resuspended in 1mL of mFreSR reagent (Stem Cell Technologies – 05855). Next, they were transferred into cryovials and stored for 24 hours at -80° C before being transferred to liquid nitrogen.

During thawing, cryovials containing iPSCs cells were thawed in a 37°C waterbath for approximately 30 seconds and transferred to a 15mL falcon tube containing 6mL of DMEM/F12 medium. Next, cells were centrifuged at 1000rpm for 5min at room temperature, and the supernatant was discarded without disturbing the cell pellet. Gently resuspend the cells in 1.5 ml of Essential 8 (E8) with 10µM Y-27632 (Tocris, cat. 1254), and then the cells were plated in solution into the vitronectin-coated well, were incubated overnight at 37 °C and 5% CO₂, and the following day the medium was refreshed with fresh Essential 8 (E8).

2.1.1. Neural crest and sensory neuron culture conditions

When the cells were ready, they were harvested using EDTA (as described above) for 15 minutes and plate at a density of 200,000 cells/cm². On the day of plating (Day 0), the cells were fed with E6 medium containing 10 µM SB431542 (Selleck Chemicals, cat, S1067), 1 ng/mL BMP4, 300 nM CHIR99021 (BioGems, cat. 2520691) and 10 µM Y-27632 (Tocris, cat. 1254). The following day (Day 1), the cells were fed with E6 medium containing 10 µM SB431542, 1 ng/mL BMP4, 300 nM CHIR99021. On Day 2 for SN induction, the cells were fed with E6 medium containing 10 mM SB431542, 0.75 mM

CHIR99021 (BioGems, cat. 2520691), 2.5 μ M SU5402, 2.5 μ M DAPT (BioGems, cat. 2088055). The medium was changed every 48hrs between day 2 and day 6.

On day 6, the cells were enzymatically dissociated with Accutase (Sigma-Aldrich, cat. A6964) for 5 minutes, washed with PBS and collected in a 15mL falcon tube. The cells were centrifuged at 1000rpm for 5 minutes at RT. The supernatant was aspirated, and the cell pellet was resuspended in neurobasal medium (Gibco, cat. 21103049) containing N2, B-27, 2 mM L-glutamine (Gibco, cat. 25030024), 20 ng/mL GDNF (PeproTech cat. 450-10), 20 ng/ mL BDNF (PeproTech cat.450-02), 25 ng/mL NGF (PeproTech cat. 450-01), 600 ng/mL laminin-1 (Sigma-Aldrich cat. L2020) and fibronectin (Corning cat. 356008), 1 μ M DAPT, 0.125 μ M retinoic acid (Sigma-Aldrich cat. R2625-50MG). The cells were counted using Countess and plated at a density of 250,000 cells/cm into PO/LM/FN-coated plates 15 mg/mL poly-L-ornithine hydrobromide (Sigma-Aldrich cat. P3655-10MG), 2 mg/mL mouse laminin-1, and 2 mg/mL human fibronectin. The medium was changed every 2-3 days through day 20. On day 20, DAPT was removed from the medium, and the medium was changed every 3-4 days.

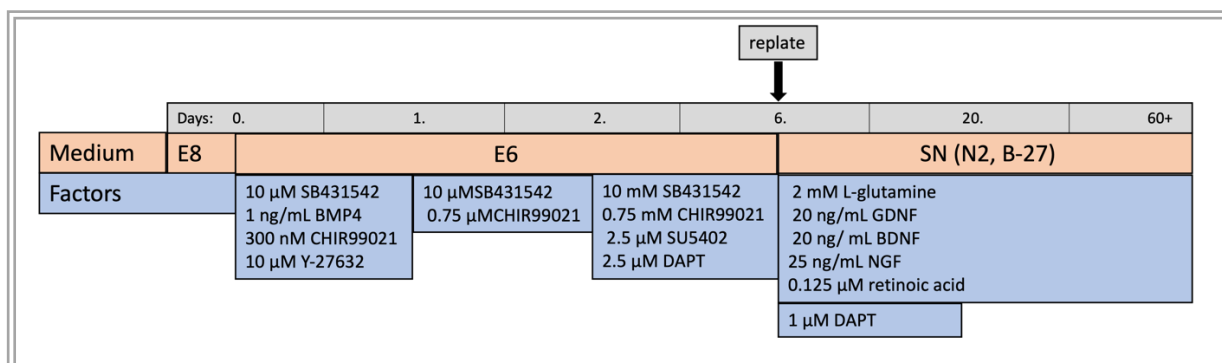


Figure 9: Protocol of differentiation

2.1.2. Immunopanning protocol

10-cm Petri dishes were coated with 40 mL of anti-mouse immunoglobulin G (IgG) or anti-goat IgG in 13 mL of 50 mM Tris-HCl (pH 9.5) at 4°C overnight. The dishes were washed three times with PBS. Incubate with 6.6 mg of TRKA, TRKB, or TRKC antibody in 5 mL of 0.2% BSA + 10 mg DNase in PBS for at least 2h at room temperature. On Day-25, SNs were washed with PBS, incubate with Accutase for 5 minutes at 37°C. Collected in PBS, and centrifuge at 1000 rpm for 5 minutes. Pellet resuspended in

Panning buffer (20% FBS, 10 mg of DNase, and 10 mM Y-27632 in PBS) (use p1000) (cells were passed through a 0.22-mm filter). The panning plates wash three times with PBS. Cells add and incubate for 15 min at room temperature and transfer to the next panning dish. Positive selection plates carefully wash with PBS seven times. The dish incubated with 5 mL of dissociation buffer (1ml of Accutase in 14 mL DMEM/F12) at 37°C for 5 minutes. Cells were dislodged with 30% FBS in 50:50 neurobasal medium/DMEM, collect, and centrifuge at 1000rpm for 5 minutes. Pellet resuspend in SN differentiation medium + 10 mM Y-27632 and plate in dried 24-well plates coated with PO/LM/FN. The medium was replaced the following day.

2.1.3. Cryostorage of SNs

For the cryostorage of SNs, the medium was removed, 1 ml of Accutase was added, and was incubated at 37 °C for approximately 5 minutes (checked regularly under microscope). Following this, 2ml of neural maintenance medium was added, and cells were pipetted up and down 3 or 4 times in the Accutase solution to achieve the dissociation of cell clumps into a single-cell suspension. The cells were collected into a 15ml falcon tube, and 2 ml of E8 was added, repeating the aforementioned step. Accutase was diluted with 4 volumes of E8, followed by centrifugation at 1000rpm for 5 minutes at room temperature to collect the cells. Subsequently, 1 ml of the resulting cell suspension was aliquoted into each cryovial. The cryovials were frozen in a CoolCell freezing container at – 80 °C overnight and later transferred to liquid nitrogen for long-term storage.

2.2. Biochemical Methods

2.2.1. Immunofluorescence assay

Cells were plated on coverslips in 6-well plates (3 coverslips per 6-well). For cell fixation, cells were washed with PBS and a 3.7% paraformaldehyde solution was added for 15minutes at room temperature. This was followed by a second wash with PBS and incubation with 50mM NH₄Cl (in PBS) for 15 minutes. Then, incubation with Triton-X 0.03% (Sigma-Aldrich cat. T8787-50ml) (in PBS) for 4 minutes was performed to

increase cell membrane permeability. Subsequently, a wash with PBS and incubation with 10% NGS for 1 hour at RT was performed to block the non-specific antigenic sites. The cells were then incubated with the primary antibody in Triton-x 0,03% in PBS, 2% NGS at 4°C overnight, (Table 4). The following day, three 5-minute washings with PBS were performed, shaking, to remove excess primary antibody. Next, the secondary antibody (GAM, GAR) diluted in PBS Triton-x 0,03%, 2% NGS was added to the coverslips for 1 hour. They were washed again with PBS thrice for 5 minutes while shaking. Then, for nuclear staining the cells were stained with Draq5 (Abcam, ab108410) in PBS 1:1000 for 15 minutes at RT. Afterwards, they were washed once with PBS and they were observed using a LeicaSP5 Confocal Microscope equipped with Argon, HeNe, 561 lasers.

2.2.2. FACS

This method is based on the characteristic scattering of light and fluorescence that every cell emits. Cells were enzymatically removed with Accutase, harvested using a scraper and transferred to new tubes with PBS enriched with 2% fetal bovine serum (FBS). Afterwards, they were centrifuged at 1000rpm for 5 minutes, and were resuspended in cold PBS with final concentration 1×10^6 cells/100mL. Antibodies labelled with fluorescent dyes (FITC-Fluorescein isothiocyanate or PE-Phycoerythrin or APC-Allophycocyanin) were added to the cells and then incubated for 1 hour in absence of light. In the present study we used TRKA, TRKB, TRKC conjugated antibodies. Consequently, 400µl PBS were added, cells were resuspended and then centrifuged for 5 minutes at 1.600rpm. Then, the supernatant was discarded, cell pellet was washed twice with PBS and incubated with DAPI (1:1,000) in 300 µl of PBS for 5 minutes. Cells were filtered and transferred to a cone-like tube of 1,5ml suitable for the FACS machine, BD FACSAria III. Analysis was carried out using the BD FACS software.

2.2.3. RNA Extraction

For the extraction of RNA, when cells were confluent as indicated, they were washed once with DMEM F12 and incubated with accutase for 5 minutes at 37°C.

Subsequently, they were dissociated and collected with DMEM F12. The cell suspension was then centrifuged at 1000rpm for 5 minutes, the supernatant was discarded, and the cell pellet was incubated with 1ml of Trizol for 5 minutes at RT. Next, 0,2ml of choroform per ml was added, shaken for 15 sec, and left to rest for 5 minutes at RT. The cell suspension was centrifuged at 12.000g for 15 minutes. The aqueous phase was carefully collected without disturbing the pellet. Then 0,5ml of 2-propanol per ml was added, shaken, and left to rest for 10 minutes at RT. The cell suspension was centrifuged at 12.000g for 10 minutes, the supernatant was discarded and the cell pellet was treated with 1ml of 75% ethanol. It was centrifuged at 7.000g for 5 minutes, the supernatant was discarded, and the pellet was left to dry by evaporating the residual ethanol. Finally, the cell pellet was collected with 40 µL of dH₂O and stored at -20°C.

The concentration of RNA in each sample was measured using a NanoDrop OneC (Thermo Fisher Scientific, Waltham, MA, USA). In parallel, its quality was assessed by the ratio of sample absorbance at 260 nm to the absorbance at 280 nm. Samples with a 260/280 ratio between 1.8-2 were considered of high purity and were further analyzed.

2.2.4. Quantitative Reverse Transcription-Polymerase Chain Reaction (RT-qPCR)

The RT-qPCR was used for the quantification of the expression of the Piezo 2 gene. It was performed in a Two-step RT-qPCR protocol using LunaScript RT SuperMix kit (NEB#E3010) and the Luna Universal qPCR Master Mix (NEB#M3003). All the components are thawed at room temperature and placed on ice due to the high proofreading activity of the enzyme leading in rapid degradation at room temperature.

Frist step:

The first step was performed to reverse transcribe the RNA to generate a cDNA library. In this step, the LunaScript® RT SuperMix Kit was used. Each sample contained 4 µL of LunaScript RT SuperMix (1x), 1 µL of RNA (concentration 1 µg), and 15 µL of Nuclease-

free Water. The samples are incubated in thermocycler (C1000 Touch Thermal Cycler - Bio-Rad) according to the cycling protocol as described below.

Table 1: Protocol for the first step of qRT-PCR

Cycling parameters of RT reaction			
CYCLE STEP	TEMPERATURE	TIME	CYCLES
Primer Annealing	25 C°	2 min	1
cDNA Synthesis	55 C°	10 min	
Heat inactivation	95 C°	1 min	

Second step:

In the second step, cDNA amplification was performed. In this step, Luna® Universal qPCR Master Mix was used. Each sample contained 10 µL of Luna Universal qPCR Master Mix (1X), 0.5 µL of the forward primer (0,25µM), 0.5 µL of the reverse primer (0,25µM), 1 µL of cDNA from the first step, and 8 µL of Nuclease-free Water. By brief centrifugation liquid is collected to the bottom of the tube and assay mix are aliquoted into qPCR tubes. PCR is performed according to the cycling protocol as described below.

Table 2: Protocol for the second step of qRT-PCR

Cycling parameters of RT- qPCR qPCR reaction			
CYCLE STEP	TEMPERATURE	TIME	CYCLES
Initial Denaturation	95C°	60 sec	1
Denaturation	95 C°	15 sec	45
Extension	60 C°	30 sec	
Melt Curve	95 C°	15sec	1

The reaction was carried out in an AriaMx RealTime PCR System, and the data were analyzed using AriaMx software. CT values were normalized against GAPDH using the equation: $2^{-\Delta Ct}$.

Table 3: Table lists the name and sequence of primers used in this report, FW: Forward, RV: Reverse

Primer Name	Primer Sequence
PIEZO2 FWD	5'GACGGACACAACCTTTGAGCCTG
PIEZO2 REV	5'CTGGCTTTGTTGGGCACTCATTG
GAPDH FWD	5' ACCACAGTCCATGCCATCAC
GAPDH REV	5'ACCACAGTCCATGCCATCAC

Table 4: Table lists of antibodies. The name of the antibodies used in this report, accompanied by information regarding clone, species, company name, catalogue number and dilution factor

Antibodies	Source	Product Code
Goat anti Mouse IgG (H+L) Cross Adsorbed Secondary Antibody, Alexa Fluor 488	ThermoFisher scientific	A-11001
Goat anti-Mouse IgG (H+L) Secondary Antibody, Alexa Fluor 568, Invitrogen	ThermoFisher scientific	A-11004
Goat anti-Rabbit IgG (H+L)Cross-Adsorbed Secondary Antibody, Alexa Fluor 488	ThermoFisher scientific	A-11008
Goat anti Rabbit IgG (H+L) Secondary Antibody, Alexa Fluor 568, Invitrogen	ThermoFisher scientific	A-11011
TrkA	R&D	MAB1751R
TrkB	R&D	MAB3971
TrkC	R&D	AF373
TUJ1	Santa cruz	sc-80005
Runx1	Sigma	HPA004176
Map2	Cell signalling	4542S
Nestin	Cell signalling	33475S
Pax6	Abcam	ab78545
TRKA-PE	R&D	FAB1751P
TRKB-AF647	R&D	FAB3971R
TRKC-PE	R&D	FAB373P
anti-mouse IgG	Jackson ImmunoResearch	115-005-003
anti-goat IgG	Jackson ImmunoResearch	705-005-003

Chapter 3

Results

3.1. Expression of characteristic markers of Sensory neurons

Induced pluripotent stem cells, XCL-1 Wt, were differentiated into Sensory neurons (SN). According to the protocol described in section 2.1. Successful differentiation was tested using three methods: morphological characterization, FACS, qRT-PCR.

During differentiation, morphological characterization of the cells was performed, and the expression of characteristic proteins expressed during differentiation was assessed. Initially, iPSCs were cultured until they reached 100% confluence, and their colonies had a circular shape; then, neural induction began (Figure 10).

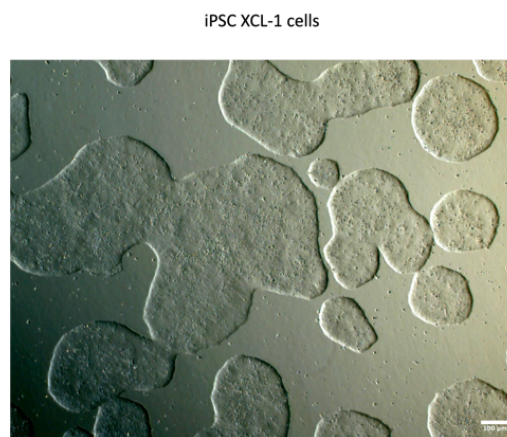


Figure 10: Images taken under optical microscope showing colonies of XCL-1 cells in mTeSRTM Plus medium and Vitronectin coated 6-well plates. Cells display a round shape and are tightly connected. 10x lens image

During the differentiation from day 0 to day 5, cells that were part of colonies were in close proximity. From day 1 to day 5, the cells transiently began to have a more elongated shape, and the peripheral cells gradually moved away from the colonies (Figure 11).

XCL-1 cells differentiated to sensory neurons Day 2

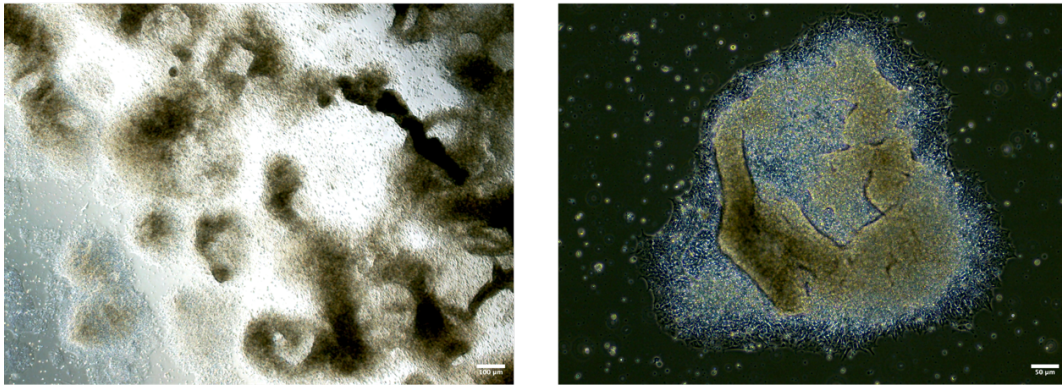


Figure 11: Images taken under optical microscope showing colonies of XCL-1 cells on day 2 of differentiation towards to sensory neurons. 4x and 20x lens image respectively

On day 6, the first replating of cells was performed. Before replating, the cells morphologically had a star-like shape and had distanced themselves significantly from the colonies (Figure 13). After replating, the cells were monolayered. Additionally, an immunofluorescence analysis was conducted for the markers Pax6 and Nestin, as it has been shown that they are expressed during the differentiation of neurons. Pax6 is a transcription factor that plays a role in the development of early neurons, while Nestin is expressed during the development of early neurons and is involved in the development of their axons. The results revealed that the cells at this stage express Pax6 and Nestin (Figure 12).

XCL-1 cells differentiated to sensory neurons Day 6

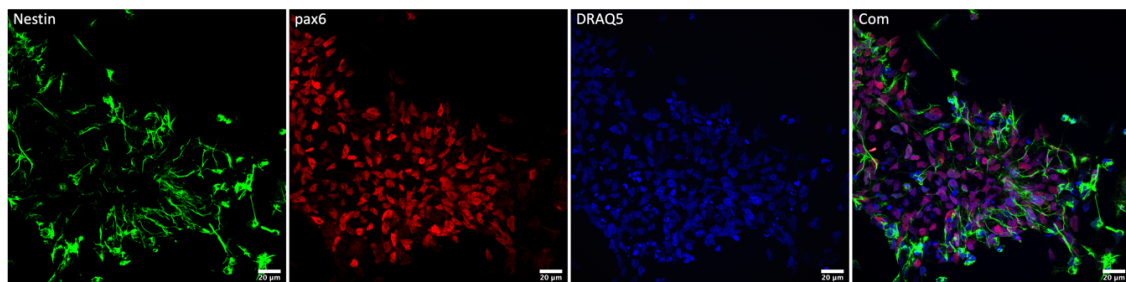


Figure 12: Expression of Pax6 and nestinon day 6 during the deafferentation of XCL-1 to sensory neurons

XCL-1 cells differentiated to sensory neurons Day 6

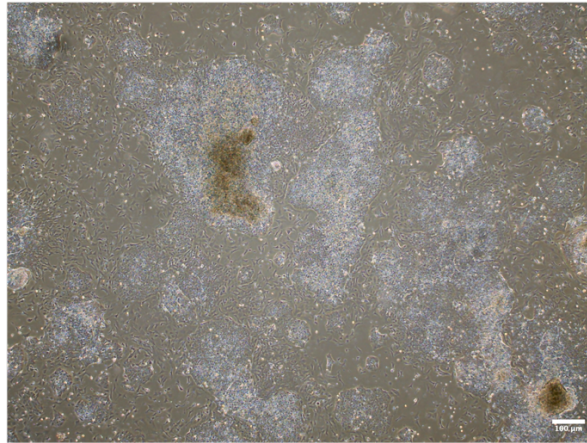


Figure 13: Image taken under optical microscope showing XCL-1 cells during differentiation. the cells start to have a star-like shape and had distanced themselves from the colonies. 4x and ens image.

On day 10, morphologically, the cells displayed neuron-like features,, cell bodies and neurites (either axonal or dendritic) were clearly visible. Subsequently, the cells were examined for the expression of markers markers Tuj1 and RunX1 using immunofluorescence. The Tuj1 protein (β II-tubulin) is a microtubulin present in the axons and dendrites of nerve cells. The RunX1 protein is expressed in TrkA cells . The analysis showed that both markers were expressed in the cells on day 10, displaying also colocalization (Figure 14) . Additionally, to examine whether the day 10 cells differentiate into all the desired sensory neuron subpopulations we examined the expression of three markers: TrkA for nociceptors, TrkB for mechanoreceptors, and TrkC for proprioceptors. Based on this, a flow cytometry analysis was performed for the three characteristic markers of sensory neurons, revealing that the day 10 cells express all three characteristic markers (Figure 15).

XCL-1 cells differentiated to sensory neurons Day 10

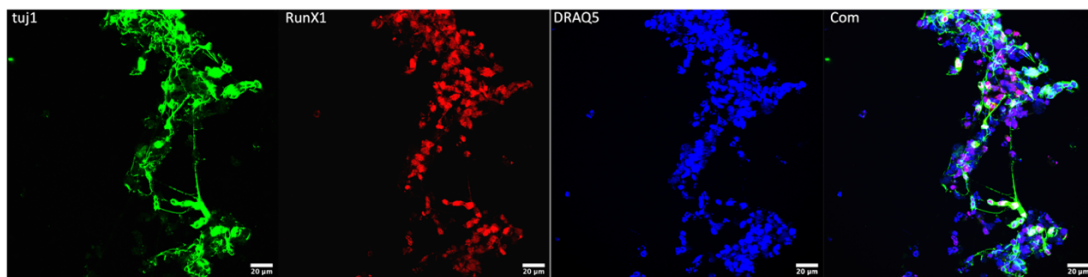


Figure 14: Expression of *tuj1* and *RunX1* on day 10 of differentiation of XCL-1 cells towards to sensory neurons

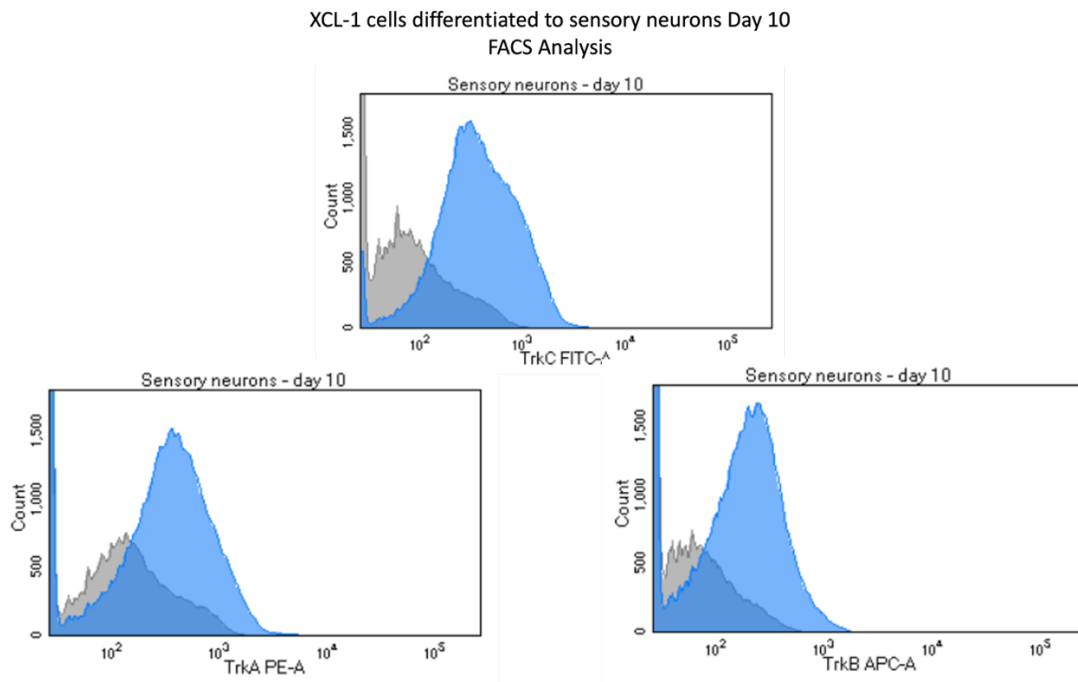


Figure 15: Expression of TrkA, TrkB, TrkC on day 10 of differentiation of XCL-1 cells to sensory neurons

On day 20, we performed the immunopanning methodology, during which we captured cells based on the membrane surface expression of the three characteristic markers TrkA, TrkB, and TrkC, corresponding to the populations we targeted to obtain with this differentiation protocol. Before the immunopanning process, all morphological analyses were conducted, and the cells had fully developed (Figure 16). Cells had the typical morphology of young sensory neurons (SN), with clearly distinguishable cell bodies, axons, and dendrites, appearing even more pronounced than the cells on day 10 (Figure 16). Additionally, to check if the cells continue to express all three markers TrkA, TrkB, and TrkC. Flow cytometry analysis was performed, revealing that all three markers were still expressed from differentiated XCL-1 cells (Figure 17). Furthermore, before the immunopanning process we performed an immunofluorescence analysis for the proteins Tuj1, RunX1, as well as for TrkB (mechanosensory neurons) and Map2. Map2 is a protein expressed in the dendrites and axons of more mature neurons, stabilizing microtubules (reference book). The results showed that Tuj1, RunX1 (Figure 18) and MAP2 and TrkB (Figure 19) were expressed in the differentiated XCL-1 cells.

XCL-1 cells differentiated to sensory neurons Day 20

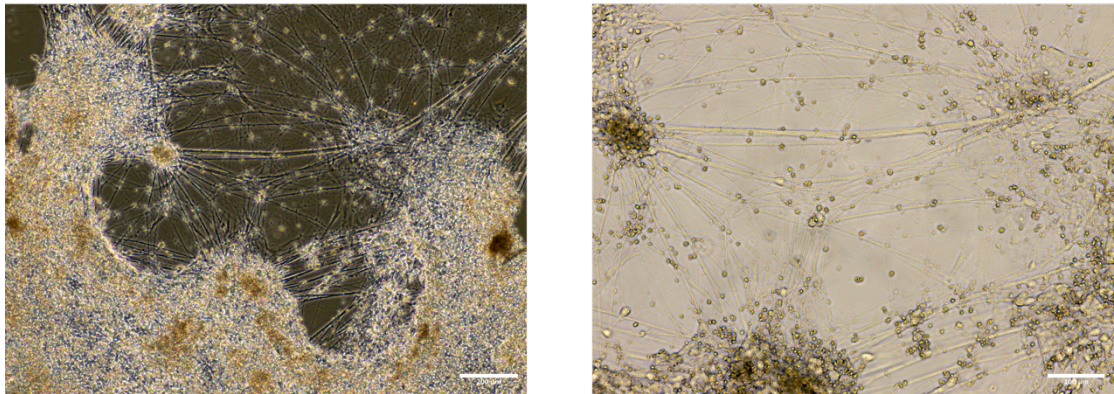


Figure 16: Images taken under optical microscope showing day 20 of differentiation for XCL-1 cells to sensory neurons. Cells had fully grown axons and dendrites. 10x and 20x lens image respectively

XCL-1 cells differentiated to sensory neurons Day 20 FACS Analysis

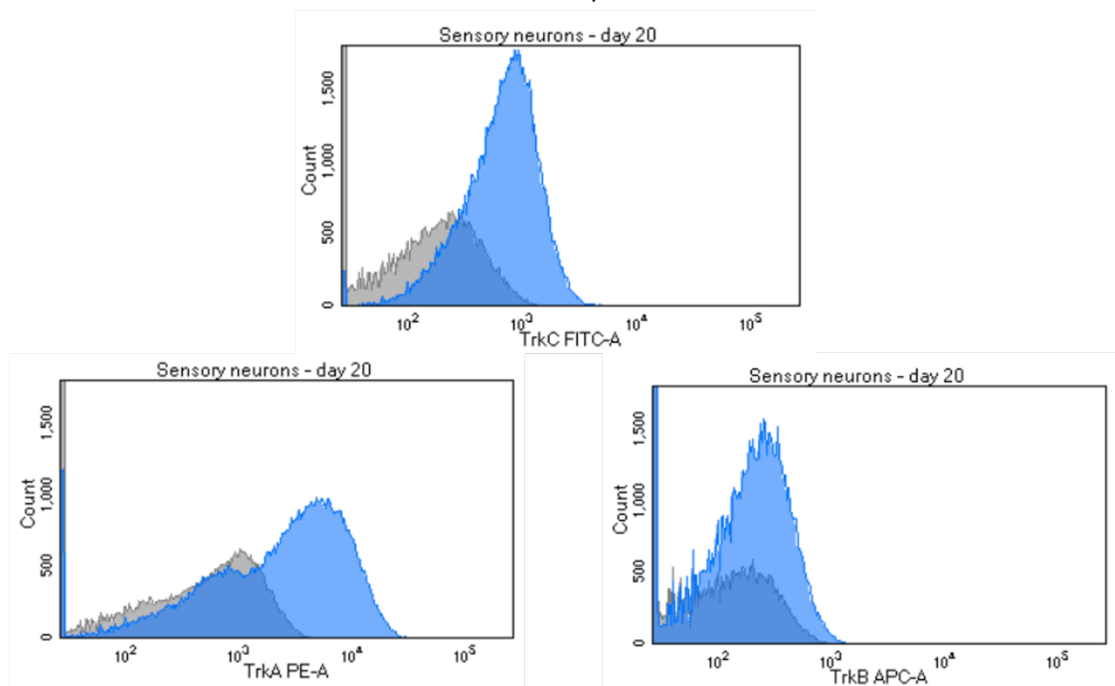


Figure 17: Expression of TrkA, TrkB, TrkC on day 20 of differentiation of XCL-1 cells to sensory neurons

XCL-1 cells differentiated to sensory neurons Day 20

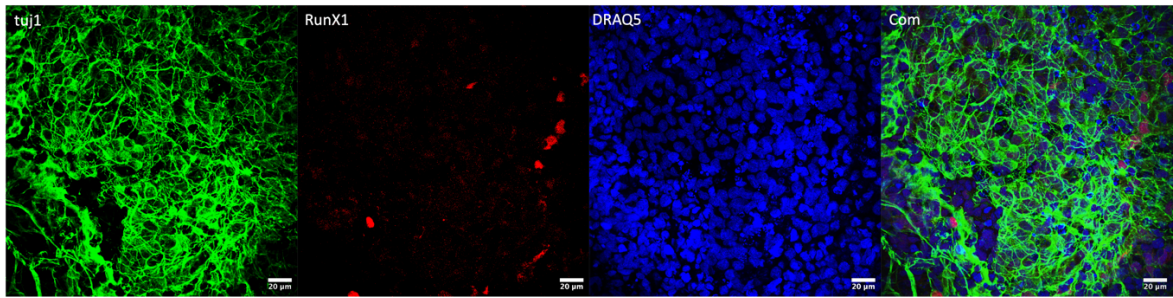


Figure 18: Expression of *tuj1* and *RunX1* on day 20 of differentiation of XCL-1 cells towards to sensory neurons

XCL-1 cells differentiated to sensory neurons Day 20

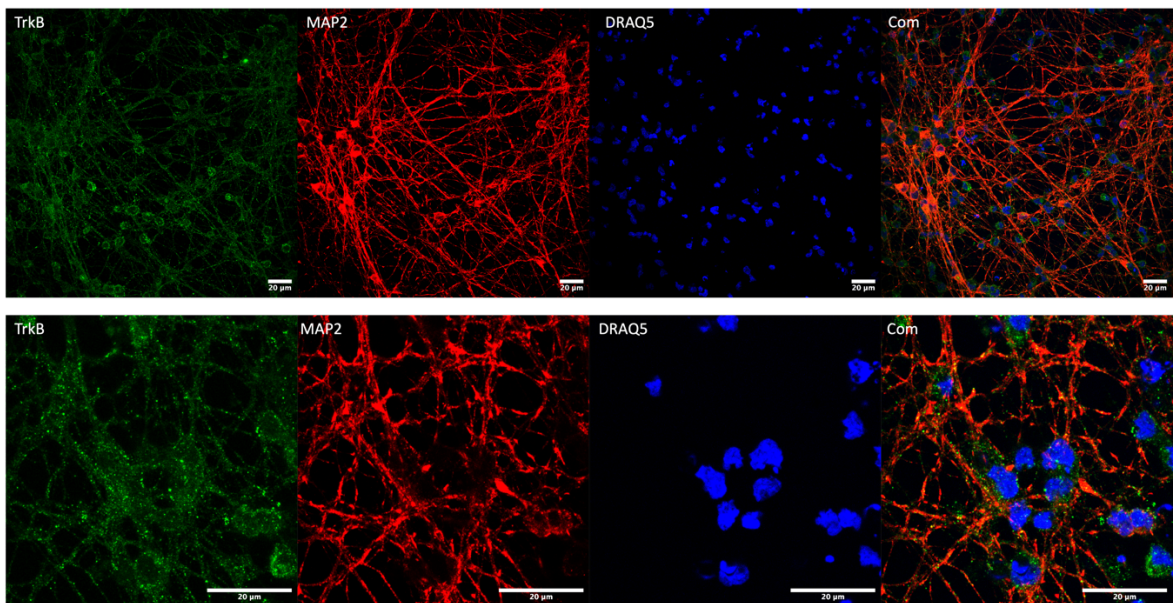


Figure 19: Expression of *TrkB* and *Map2* on day 20 of differentiation of XCL-1 cells towards to sensory neurons

On day 65, the differentiated XCL-1 cells had developed fully after immunopanning and their structure was clearly visible, resembling mature sensory neurons (Figure 21). Subsequently, we examined *TrkB* expression using immunofluorescence to determine if we achieved the generation of mechanoreceptors. The analysis revealed that there was prominent expression of *TrkB* (Figure 20).

XCL-1 cells differentiated to sensory neurons Day 20

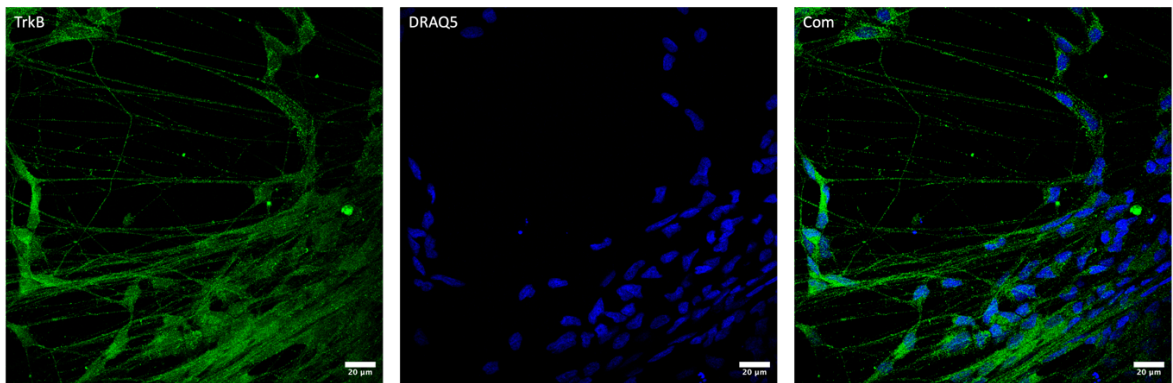


Figure 20: Expression of TrkB and on day 65 of differentiation of XCL-1 cells towards to mechanosensory neurons

XCL-1 cells differentiated to sensory neurons Day 65

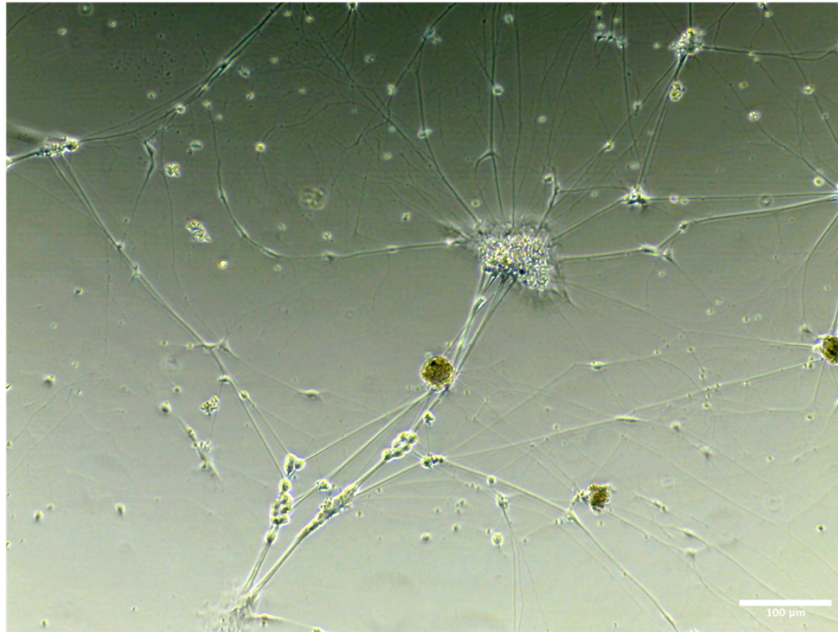


Figure 21: Images taken under optical microscope showing day 65 of differentiation for XCL-1 cells to sensory neurons. Cells had fully grown axons and dendrites. 20x lens image respectively

3.2. Expression of Piezo2 to XCL-1 during differentiation

Piezo 2 is a gene that is primarily expressed in mechanoreceptors (TrkB cells). To examine the expression of the Piezo2 mRNA, we performed RT-qPCR at various time points during the differentiation of sensory neurons. mRNA isolation was performed at 10 and 20 days after differentiation, as well as after the immunopanning for the three populations (TrkA, TrkB, TrkC) on day 65. We detected a significant difference ($p=0,0001$) in the expression of Piezo2 in the sensory receptors on day 10 and in TrkA sensory receptors on day 65 ($p=0,01$) when compared to the population of mature TrkB cells on day 65. However, no significant difference in the expression of Piezo2 was observed in the sensory neurons on day 20 ($p=0,9$) and in TrkC sensory neurons on day 65 compared to the sensory neurons TrkB on day 65 ($p=0,9$ (Figure 22).

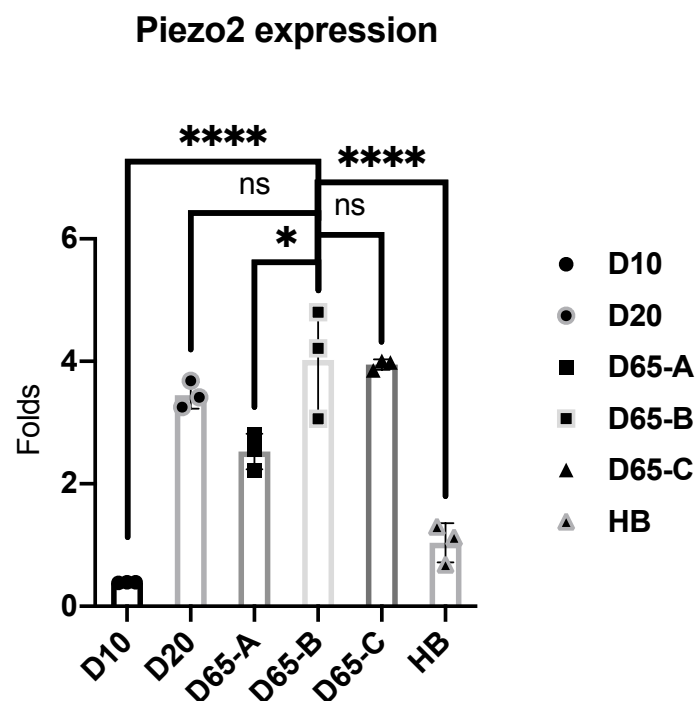


Figure 22: Expression of Piezo2 in different time point during the differentiation of XCL-1 cells to sensory neurons.

D10: $\pm 0,02$ SEM, D20 $\pm 0,12$ SEM, D65-A $\pm 0,16$ SEM, D65-B $\pm 0,4$ SEM, D65-C $\pm 0,04$ SEM, HB $\pm 0,1$ SEM

Chapter 4

Discussion

In this specific research, our focus was on the differentiation and maturation of sensory neurons (nociceptors, mechanoreceptors, proprioceptors) from induced Pluripotent Stem Cells (iPSCs), focusing on mechanoreceptors. The goal was to establish a protocol for differentiating induced Pluripotent Stem Cells into sensory neurons, with the subsequent aim of studying the mTOR pathway in mechanoreceptors and how touch is affected in individuals with Autism Spectrum Disorder (ASD).

Collaborative work from the Gkogkas lab revealed that 4E-BP1 deletion in mice leads to mechanical, but not thermal hypersensitivity, suggesting that the mTORC1/4E-BP1 axis is critical for tactile sensation (Khoutorsky et al., 2015b). Furthermore, recently the Gkogkas lab revealed regulation of a subset of mRNAs in mechanosensory cells downstream of mTORC1/4E-BP1. These new results show that mTORC1 promotes sensory hypersensitivity via 4E-BP1-dependent up-regulation of tripartite motif-containing protein 32 (TRIM32)/interferon signaling and identify TRIM32 as a potential therapeutic target. (Wong et al., 2023)

There are several published protocols that describe sensory neuron induction from iPSCs – given our goal we focused on achieving a high percentage of successfully differentiated mechanoreceptors. Some protocols derive sensory neurons from spheroids (Schrenk-Siemens et al., 2015) or achieve a small percentage of mechanoreceptors (Guo et al., 2013). For all these reasons, our preparation was based on (Saito-Diaz et al., 2021) protocol.

Due to time limitations, we cultured the cells only up to day 65 after the neural induction. After neural induction from day 0 until day 6, the differentiation rate is increased due to the growth factors present in the culture medium. In Day 6 we replated the differentiated XCL-1 cells, a manipulation which was shown to increase the percentage of mechanoreceptors based on the Saito-Diaz et al protocol. At this point the cells did not form scattered colonies, they were smaller and aggregated.

From day 6 small extensions of axons and dendrites appeared and up until day 20 we observed prominent dendrites and axons, hallmarks of neuronal morphology. Additionally, a clearly shaped soma of these neurons was visible. Importantly, we observed unipolar neuron morphology, which is typical of sensory neurons with cell bodies in the spinal nerve ganglia, further supporting successful differentiation into this cell type from human iPSC (XCL-1). On day 20 we performed the immunopanning in order to separate the differentiated XCL-1 cells in three populations of (nociceptors, mechanoreceptors, proprioceptors) based on the three characteristic markers that this type of cells are expressed TrkA, TrkB, TrkC respectively.

We wanted to examine whether cells express specific markers at specific time points to monitor their progression towards sensory neurons. Thus, at the first time point on day 6, we checked the expression of Pax6 and Nestin. Differentiated XCL-1 cells appeared to express both markers. The expression of these markers indicates that differentiated XCL-1 cells have moved towards neurons, as these markers are expressed in neural crest cells (NCC). The next time point we examined the expression of Tuj1 and Runx1 on day 10. We chose these markers to investigate if cells have started to differentiate into sensory neurons, specifically nociceptors, as Runx1 is a characteristic marker of nociceptors. As shown earlier, differentiated XCL-1 cells expressed both markers, leading us to conclude that the cells have passed the NCC stage and are progressing towards sensory neurons. On day 20, we analyzed the expression of characteristic markers for sensory neurons, namely Tuj1 in combination with RunX1 and TrkB with Map2. Tuj1-Runx1 were examined on Day10 and are indicative of this timepoint in the differentiation as shown in the Saito-Diaz et al. protocol. TRkB-Map2 were examined to investigate whether XCL-1 cells differentiated into mechanoreceptors, as TrkB is a characteristic molecule expressed in this type of sensory neuron. Map2 is a marker expressed in most mature neurons, and its expression at this stage revealed that neurons have matured. Finally, we examined the expression of TrkB on day 65. We chose this specific marker because the goal of differentiating XCL-1 cells was to obtain an enriched population of TrkB cells. The marker was strongly expressed in immunopanned cells (>90% of cells in the plate),

indicating that the differentiation was successful. A future goal is to examine all the mentioned markers at all time points for the protocols to correlate marker expression with earlier developmental stages. Additionally, other characteristic markers such as RunX3, expressed in early mechanoreceptors and proprioceptors, should be examined. Another crucial molecule in the maturation of all sensory neurons is BRN3A, and its expression should be analyzed throughout the differentiation process.

An additional analysis we conducted to ascertain whether differentiated XCL-1 cells had committed towards sensory neurons was flow cytometry for the markers TrkA, TrkB, and TrkC, characteristic for nociceptors, mechanoreceptors, and proprioceptors, respectively. Day 10 was the first day of this particular analysis, revealing that the cells had started to differentiate in the correct direction. On day 20, a confirmatory experiment for the same markers was performed, validating the expression of all three markers in the mixed cell population before isolating the three populations based on these Trk surface receptors. In the future, we need to further monitor the expression of Trk markers from the beginning of differentiation to better characterize the dynamics of differentiation.

The main goal of our differentiation protocol was focused on mechanoreceptors; a cardinal molecule expressed in these cells is Piezo-type mechanosensitive ion channel component 2 (Piezo2). For this reason, we measured mRNA expression using RT-qPCR. Piezo2 expression was significantly increased in differentiated mechanoreceptors compared with differentiated XCL-1 cells on day 10 and from nociceptors on day 65. However, on day 20, when all populations were combined from the differentiated XCL-1 cells, there was no statistical significance, and the same was observed for proprioceptors. This analysis strengthened our conclusion that the differentiation was successful.

In the future, we should continue to culture the differentiated cells until day 90 to observe the expression of characteristic markers and achieve more mature stages in sensory neuron development. This extended timeframe will allow us to further strengthen the evidence that the cells are progressing towards sensory neurons and display mature physiological phenotypes (e.g. electrophysiological).

To investigate the initial hypothesis, differentiation needs to be carried out in cells where there is the deletion of a gene associated with Autism Spectrum Disorder (ASD), such as PTEN, impacting the mTOR pathway. This would enable us to monitor the pathway and examine the changes it would induce in translational control.

References

- Avilion, A. A., Nicolis, S. K., Pevny, L. H., Perez, L., Vivian, N., & Lovell-Badge, R. (2003). Multipotent cell lineages in early mouse development depend on SOX2 function. *Genes and Development*, 17(1), 126–140. <https://doi.org/10.1101/gad.224503>
- Baranek, G. T., David, F. J., Poe, M. D., Stone, W. L., & Watson, L. R. (2006). Sensory Experiences Questionnaire: Discriminating sensory features in young children with autism, developmental delays, and typical development. *Journal of Child Psychology and Psychiatry and Allied Disciplines*, 47(6), 591–601. <https://doi.org/10.1111/j.1469-7610.2005.01546.x>
- Ben-Sasson, A., Cermak, S. A., Orsmond, G. I., Tager-Flusberg, H., Kadlec, M. B., & Carter, A. S. (2008). Sensory clusters of toddlers with autism spectrum disorders: Differences in affective symptoms. *Journal of Child Psychology and Psychiatry and Allied Disciplines*, 49(8), 817–825. <https://doi.org/10.1111/j.1469-7610.2008.01899.x>
- Bhavanasi, D., & Klein, P. S. (2016). Wnt Signaling in Normal and Malignant Stem Cells. In *Current Stem Cell Reports* (Vol. 2, Issue 4, pp. 379–387). Springer International Publishing. <https://doi.org/10.1007/s40778-016-0068-y>
- Boyer, L. A., Tong, I. L., Cole, M. F., Johnstone, S. E., Levine, S. S., Zucker, J. P., Guenther, M. G., Kumar, R. M., Murray, H. L., Jenner, R. G., Gifford, D. K., Melton, D. A., Jaenisch, R., & Young, R. A. (2005). Core transcriptional regulatory circuitry in human embryonic stem cells. *Cell*, 122(6), 947–956. <https://doi.org/10.1016/j.cell.2005.08.020>
- campbell1996*. (n.d.).
- cdf370*. (n.d.).
- Chambers, I., Silva, J., Colby, D., Nichols, J., Nijmeijer, B., Robertson, M., Vrana, J., Jones, K., Grotewold, L., & Smith, A. (2007). Nanog safeguards pluripotency and mediates germline development. *Nature*, 450(7173), 1230–1234. <https://doi.org/10.1038/nature06403>
- Chambers, I., & Smith, A. (2004). Self-renewal of teratocarcinoma and embryonic stem cells. In *Oncogene* (Vol. 23, Issue 43 REV. ISS. 6, pp. 7150–7160). <https://doi.org/10.1038/sj.onc.1207930>
- Chen, C. L., Broom, D. C., Liu, Y., De Noij, J. C., Li, Z., Cen, C., Samad, O. A., Jessell, T. M., Woolf, C. J., & Ma, Q. (2006). Runx1 determines nociceptive sensory neuron phenotype and is required for thermal and neuropathic pain. *Neuron*, 49(3), 365–377. <https://doi.org/10.1016/j.neuron.2005.10.036>
- chung1992*. (n.d.).
- Dailey, L., Ambrosetti, D., Mansukhani, A., & Basilico, C. (2005). Mechanisms underlying differential responses to FGF signaling. *Cytokine and Growth Factor Reviews*, 16(2 SPEC. ISS.), 233–247. <https://doi.org/10.1016/j.cytogfr.2005.01.007>
- Darnell, J. C., Van Driesche, S. J., Zhang, C., Hung, K. Y. S., Mele, A., Fraser, C. E., Stone, E. F., Chen, C., Fak, J. J., Chi, S. W., Licatalosi, D. D., Richter, J. D., & Darnell, R. B. (2011). FMRP stalls ribosomal translocation on mRNAs linked to synaptic function and autism. *Cell*, 146(2), 247–261. <https://doi.org/10.1016/j.cell.2011.06.013>

- Elison, J. T., Paterson, S. J., Wolff, J. J., Steven Reznick, J., Sasson, N. J., Gu, H., Botteron, K. N., Dager, S. R., Estes, A. M., Evans, A. C., Gerig, G., Hazlett, H. C., Schultz, R. T., Styner, M., Zwaigenbaum, L., & Piven, J. (n.d.). *White Matter Microstructure and Atypical Visual Orienting in 7-Month-Olds at Risk for Autism*.
- Fedtsova, N., Perris, R., & Turner, E. E. (2003). Sonic hedgehog regulates the position of the trigeminal ganglia. *Developmental Biology*, 261(2), 456–469. [https://doi.org/10.1016/S0012-1606\(03\)00316-6](https://doi.org/10.1016/S0012-1606(03)00316-6)
- Functional Expression Cloning of Nanog, a Pluripotency Sustaining Factor in Embryonic Stem Cells*. (n.d.). <http://smart.embl-heidelberg.de>
- Gingras, A.-C., Raught, B., & Sonenberg, N. (1999). eIF4 INITIATION FACTORS: EFFECTORS OF mRNA RECRUITMENT TO RIBOSOMES AND REGULATORS OF TRANSLATION. In *Annu. Rev. Biochem* (Vol. 68). www.annualreviews.org
- Gkogkas, C. G., Khoutorsky, A., Ran, I., Rampakakis, E., Nevarko, T., Weatherill, D. B., Vasuta, C., Yee, S., Truitt, M., Dallaire, P., Major, F., Lasko, P., Ruggero, D., Nader, K., Lacaille, J. C., & Sonenberg, N. (2013). Autism-related deficits via dysregulated eIF4E-dependent translational control. *Nature*, 493(7432), 371–377. <https://doi.org/10.1038/nature11628>
- Green, S. A., Ben-Sasson, A., Soto, T. W., & Carter, A. S. (2012). Anxiety and sensory over-responsivity in toddlers with autism spectrum disorders: Bidirectional effects across time. *Journal of Autism and Developmental Disorders*, 42(6), 1112–1119. <https://doi.org/10.1007/s10803-011-1361-3>
- Grifo, J. A., Tahara, S. M., Morgan, M. A., Shatkin, A. J., & Merrick, W. C. (1983). New initiation factor activity required for globin mRNA translation. *Journal of Biological Chemistry*, 258(9), 5804–5810. [https://doi.org/10.1016/s0021-9258\(20\)81965-6](https://doi.org/10.1016/s0021-9258(20)81965-6)
- Guo, X., Spradling, S., Stancescu, M., Lambert, S., & Hickman, J. J. (2013). Derivation of sensory neurons and neural crest stem cells from human neural progenitor hNP1. *Biomaterials*, 34(18), 4418–4427. <https://doi.org/10.1016/j.biomaterials.2013.02.061>
- Hagerman, R. J., Berry-Kravis, E., Hazlett, H. C., Bailey, D. B., Moine, H., Kooy, R. F., Tassone, F., Gantois, I., Sonenberg, N., Mandel, J. L., & Hagerman, P. J. (2017). Fragile X syndrome. *Nature Reviews Disease Primers*, 3(1). <https://doi.org/10.1038/NRDP.2017.65>
- Hay, N., & Sonenberg, N. (2004). Upstream and downstream of mTOR. In *Genes and Development* (Vol. 18, Issue 16, pp. 1926–1945). <https://doi.org/10.1101/gad.1212704>
- Hirai, H., Tani, T., Katoku-Kikyo, N., Kellner, S., Karian, P., Firpo, M., & Kikyo, N. (2011). Radical acceleration of nuclear reprogramming by chromatin remodeling with the transactivation domain of MyoD. *Stem Cells*, 29(9), 1349–1361. <https://doi.org/10.1002/stem.684>
- Hochedlinger, K., & Jaenisch, R. (2006). Nuclear reprogramming and pluripotency. In *Nature* (Vol. 441, Issue 7097, pp. 1061–1067). Nature Publishing Group. <https://doi.org/10.1038/nature04955>
- Hwang, Y., Kim, L. C., Song, W., Edwards, D. N., Cook, R. S., & Chen, J. (2019). Disruption of the scaffolding function of mLST8 selectively inhibits mTORC2 assembly and function and suppresses mTORC2-dependent tumor growth in

- vivo. *Cancer Research*, 79(13), 3178–3184. <https://doi.org/10.1158/0008-5472.CAN-18-3658>
- Iarocci, G., & McDonald, J. (2006). Sensory integration and the perceptual experience of persons with autism. *Journal of Autism and Developmental Disorders*, 36(1), 77–90. <https://doi.org/10.1007/s10803-005-0044-3>
- Jacinto, E., Loewith, R., Schmidt, A., Lin, S., Rügge, M. A., Hall, A., & Hall, M. N. (2004). Mammalian TOR complex 2 controls the actin cytoskeleton and is rapamycin insensitive. *Nature Cell Biology*, 6(11), 1122–1128. <https://doi.org/10.1038/ncb1183>
- kamachi2000. (n.d.).
- Khoutorsky, A., Bonin, R. P., Sorge, R. E., Gkogkas, C. G., Anne Pawlowski, S., Mehdi Jafarnejad, S., Pitcher, M. H., Alain, T., Perez-Sanchez, J., Salter, E. W., Martin, L., Ribeiro-da-Silva, A., De Koninck, Y., Cervero, F., Mogil, J. S., & Sonenberg, N. (2015a). *Translational control of nociception via 4E-binding protein 1*. <https://doi.org/10.7554/eLife.12002.001>
- Khoutorsky, A., Bonin, R. P., Sorge, R. E., Gkogkas, C. G., Anne Pawlowski, S., Mehdi Jafarnejad, S., Pitcher, M. H., Alain, T., Perez-Sanchez, J., Salter, E. W., Martin, L., Ribeiro-da-Silva, A., De Koninck, Y., Cervero, F., Mogil, J. S., & Sonenberg, N. (2015b). *Translational control of nociception via 4E-binding protein 1*. <https://doi.org/10.7554/eLife.12002.001>
- Kilpinen, H., Goncalves, A., Leha, A., Afzal, V., Alasoo, K., Ashford, S., Bala, S., Bensaddek, D., Casale, F. P., Culley, O. J., Danecek, P., Faulconbridge, A., Harrison, P. W., Kathuria, A., McCarthy, D., McCarthy, S. A., Meleckyte, R., Memari, Y., Moens, N., ... Gaffney, D. J. (2017). Common genetic variation drives molecular heterogeneity in human iPSCs. *Nature*, 546(7658), 370–375. <https://doi.org/10.1038/nature22403>
- Kim, S. G., Buel, G. R., & Blenis, J. (2013). Nutrient regulation of the mTOR complex 1 signaling pathway. In *Molecules and cells* (Vol. 35, Issue 6, pp. 463–473). <https://doi.org/10.1007/s10059-013-0138-2>
- Klintwall, L., Holm, A., Eriksson, M., Carlsson, L. H., Olsson, M. B., Hedvall, Å., Gillberg, C., & Fernell, E. (2011). Sensory abnormalities in autism. A brief report. *Research in Developmental Disabilities*, 32(2), 795–800. <https://doi.org/10.1016/j.ridd.2010.10.021>
- Kojovic, N., Hadid, L. Ben, Franchini, M., & Schaer, M. (2019). Sensory processing issues and their association with social difficulties in children with Autism spectrum disorders. *Journal of Clinical Medicine*, 8(10). <https://doi.org/10.3390/jcm8101508>
- Koyanagi-Aoi, M., Ohnuki, M., Takahashi, K., Okita, K., Noma, H., Sawamura, Y., Teramoto, I., Narita, M., Sato, Y., Ichisaka, T., Amano, N., Watanabe, A., Morizane, A., Yamada, Y., Sato, T., Takahashi, J., & Yamanaka, S. (2013). Differentiation-defective phenotypes revealed by large-scale analyses of human pluripotent stem cells. *Proceedings of the National Academy of Sciences of the United States of America*, 110(51), 20569–20574. <https://doi.org/10.1073/pnas.1319061110>
- Levanon, D., Brenner, O., Negreanu, V., Bettoun, D., Woolf, E., Eilam, R., Lotem, J., Gat, U., Otto, F., Speck, N., & Groner, Y. (n.d.). *Spatial and temporal expression*

- pattern of Runx3 (Aml2) and Runx1 (Aml1) indicates non-redundant functions during mouse embryogenesis.* www.elsevier.com/locate/mode
- Li, J., Wang, G., Wang, C., Zhao, Y., Zhang, H., Tan, Z., Song, Z., Ding, M., & Deng, H. (2007). MEK/ERK signaling contributes to the maintenance of human embryonic stem cell self-renewal. *Differentiation*, 75(4), 299–307. <https://doi.org/10.1111/j.1432-0436.2006.00143.x>
- Liu, G. Y., & Sabatini, D. M. (2020). mTOR at the nexus of nutrition, growth, ageing and disease. In *Nature Reviews Molecular Cell Biology* (Vol. 21, Issue 4, pp. 183–203). Nature Research. <https://doi.org/10.1038/s41580-019-0199-y>
- Logan, C. Y., & Nusse, R. (2004). The Wnt signaling pathway in development and disease. In *Annual Review of Cell and Developmental Biology* (Vol. 20, pp. 781–810). <https://doi.org/10.1146/annurev.cellbio.20.010403.113126>
- Loh, K. M., & Lim, B. (2011). A precarious balance: Pluripotency factors as lineage specifiers. In *Cell Stem Cell* (Vol. 8, Issue 4, pp. 363–369). <https://doi.org/10.1016/j.stem.2011.03.013>
- Marmigère, F., Montelius, A., Wegner, M., Groner, Y., Reichardt, L. F., & Ernfors, P. (2006). The Runx1/AML1 transcription factor selectively regulates development and survival of TrkA nociceptive sensory neurons. *Nature Neuroscience*, 9(2), 180–187. <https://doi.org/10.1038/nn1631>
- Masui, S., Nakatake, Y., Toyooka, Y., Shimosato, D., Yagi, R., Takahashi, K., Okochi, H., Okuda, A., Matoba, R., Sharov, A. A., Ko, M. S. H., & Niwa, H. (2007). Pluripotency governed by Sox2 via regulation of Oct3/4 expression in mouse embryonic stem cells. *Nature Cell Biology*, 9(6), 625–635. <https://doi.org/10.1038/ncb1589>
- Mitalipov, S., & Wolf, D. (2009). Totipotency, pluripotency and nuclear reprogramming. *Advances in Biochemical Engineering/Biotechnology*, 114, 185–199. https://doi.org/10.1007/10_2008_45
- Moessner, R., Marshall, C. R., Sutcliffe, J. S., Skaug, J., Pinto, D., Vincent, J., Zwaigenbaum, L., Fernandez, B., Roberts, W., Szatmari, P., & Scherer, S. W. (2007). Contribution of SHANK3 mutations to autism spectrum disorder. *American Journal of Human Genetics*, 81(6), 1289–1297. <https://doi.org/10.1086/522590>
- Niwa, H., Burdon, T., Chambers, I., & Smith, A. (1998). *Self-renewal of pluripotent embryonic stem cells is mediated via activation of STAT3.* www.genesdev.org
- Niwa, H., Miyazaki, J.-I., & Smith, A. G. (2000). *Quantitative expression of Oct-3/4 defines differentiation, dedifferentiation or self-renewal of ES cells.* http://genetics.nature.com/supplementary_info/
- Orefice, L. L. L., Zimmerman, A. L. L., Chirila, A. M. M., Sleboda, S. J. J., Head, J. P. P., & Ginty, D. D. D. (2016). Peripheral Mechanosensory Neuron Dysfunction Underlies Tactile and Behavioral Deficits in Mouse Models of ASDs. *Cell*, 166(2), 299–313. <https://doi.org/10.1016/j.cell.2016.05.033>
- Orefice, L. L., Mosko, J. R., Morency, D. T., Wells, M. F., Tasnim, A., Mozeika, S. M., Ye, M., Chirila, A. M., Emanuel, A. J., Rankin, G., Fame, R. M., Lehtinen, M. K., Feng, G., & Ginty, D. D. (2019). Targeting Peripheral Somatosensory Neurons to Improve Tactile-Related Phenotypes in ASD Models. *Cell*, 178(4), 867–886.e24. <https://doi.org/10.1016/j.cell.2019.07.024>

- Park, K.-S. (2011). TGF-beta Family Signaling in Embryonic Stem Cells. In *International Journal of Stem Cells* (Vol. 4, Issue 1).
- Peterson, T. R., Laplante, M., Thoreen, C. C., Sancak, Y., Kang, S. A., Kuehl, W. M., Gray, N. S., & Sabatini, D. M. (2009). DEPTOR Is an mTOR Inhibitor Frequently Overexpressed in Multiple Myeloma Cells and Required for Their Survival. *Cell*, 137(5), 873–886. <https://doi.org/10.1016/j.cell.2009.03.046>
- Peterson, T. R., Sengupta, S. S., Harris, T. E., Carmack, A. E., Kang, S. A., Balderas, E., Guertin, D. A., Madden, K. L., Carpenter, A. E., Finck, B. N., & Sabatini, D. M. (2011). MTOR complex 1 regulates lipin 1 localization to control the srebp pathway. *Cell*, 146(3), 408–420. <https://doi.org/10.1016/j.cell.2011.06.034>
- Raisz Eng, S., Dykes, I. M., Lanier, J., Fedtsova, N., & Turner, E. E. (2007). POU-domain factor Brn3a regulates both distinct and common programs of gene expression in the spinal and trigeminal sensory ganglia. *Neural Development*, 2(1). <https://doi.org/10.1186/1749-8104-2-3>
- Robertson, E. J., Norris, D. P., Brennan, J., Bikoff, E. K., & Gardner, R. L. (2003). Control of early anterior-posterior patterning in the mouse embryo by TGF- β signalling. In *Philosophical Transactions of the Royal Society B: Biological Sciences* (Vol. 358, Issue 1436, pp. 1351–1358). Royal Society. <https://doi.org/10.1098/rstb.2003.1332>
- Rogers, S. J., Hepburn, S., & Wehner, E. (2003). Parent Reports of Sensory Symptoms in Toddlers with Autism and Those with Other Developmental Disorders. In *Journal of Autism and Developmental Disorders* (Vol. 33, Issue 6).
- Saito-Diaz, K., Street, J. R., Ulrichs, H., & Zeltner, N. (2021). Derivation of Peripheral Nociceptive, Mechanoreceptive, and Proprioceptive Sensory Neurons from the same Culture of Human Pluripotent Stem Cells. *Stem Cell Reports*, 16(3), 446–457. <https://doi.org/10.1016/j.stemcr.2021.01.001>
- Scholer, H. R., Hatzopoulos, A. K., Balling, R., Suzuki, N., & Gruss, P. (1989). A family of octamer-specific proteins present during mouse embryogenesis: evidence for germline-specific expression of an Oct factor. *EMBO Journal*, 8(9), 2543–2550. <https://doi.org/10.1002/j.1460-2075.1989.tb08392.x>
- Schrenk-Siemens, K., Wende, H., Prato, V., Song, K., Rostock, C., Loewer, A., Utikal, J., Lewin, G. R., Lechner, S. G., & Siemens, J. (2015). PIEZO2 is required for mechanotransduction in human stem cell-derived touch receptors. *Nature Neuroscience*, 18(1), 10–16. <https://doi.org/10.1038/nn.3894>
- Schwanhüsser, B., Busse, D., Li, N., Dittmar, G., Schuchhardt, J., Wolf, J., Chen, W., & Selbach, M. (2011). Global quantification of mammalian gene expression control. *Nature*, 473(7347), 337–342. <https://doi.org/10.1038/nature10098>
- Silva, J., & Smith, A. (2008). Capturing Pluripotency. In *Cell* (Vol. 132, Issue 4, pp. 532–536). Elsevier B.V. <https://doi.org/10.1016/j.cell.2008.02.006>
- Sonenberg, N., Rupprecht, K. M., Hecht, S. M., & Shatkin, A. J. (1979). Eukaryotic mRNA cap binding protein: Purification by affinity chromatography on Sepharose-coupled m7GDP (7-methylguanosine/eukaryotic initiation factors/protein synthesis). In *Biochemistry* (Vol. 76, Issue 9).
- Sullivan, J. C., Miller, L. J., Nielsen, D. M., & Schoen, S. A. (2014). The presence of migraines and its association with sensory hyperreactivity and anxiety symptomatology in children with autism spectrum disorder. *Autism*, 18(6), 743–747. <https://doi.org/10.1177/1362361313489377>

- Takahashi, K., Tanabe, K., Ohnuki, M., Narita, M., Ichisaka, T., Tomoda, K., & Yamanaka, S. (2007). Induction of Pluripotent Stem Cells from Adult Human Fibroblasts by Defined Factors. *Cell*, 131(5), 861–872. <https://doi.org/10.1016/j.cell.2007.11.019>
- Takahashi, K., & Yamanaka, S. (2006). Induction of Pluripotent Stem Cells from Mouse Embryonic and Adult Fibroblast Cultures by Defined Factors. *Cell*, 126(4), 663–676. <https://doi.org/10.1016/j.cell.2006.07.024>
- Tavassoli, T., Miller, L. J., Schoen, S. A., Nielsen, D. M., & Baron-Cohen, S. (2014). Sensory over-responsivity in adults with autism spectrum conditions. *Autism*, 18(4), 428–432. <https://doi.org/10.1177/1362361313477246>
- Theriault, F. M., Roy, P., & Stifani, S. (2004). *AML1Runx1 is important for the development of hindbrain cholinergic branchiovisceral motor neurons and selected cranial sensory neurons*. www.pnas.org/cgi/doi/10.1073/pnas.0400768101
- Unni, N., & Arteaga, C. L. (2019). Is Dual mTORC1 and mTORC2 Therapeutic Blockade Clinically Feasible in Cancer? In *JAMA Oncology* (Vol. 5, Issue 11, pp. 1564–1565). American Medical Association. <https://doi.org/10.1001/jamaoncol.2019.2525>
- Vallier, L., Mendjan, S., Brown, S., Ching, Z., Teo, A., Smithers, L. E., Trotter, M. W. B., Cho, C. H. H., Martinez, A., Rugg-Gunn, P., Brons, G., & Pedersen, R. A. (2009). Activin/Nodal signalling maintains pluripotency by controlling Nanog expression. *Development*, 136(8), 1339–1349. <https://doi.org/10.1242/dev.033951>
- Vezina, C., Kudelski, A., & Sehgal, S. N. (n.d.). *RAPAMYCIN (AY-22,989), A NEW ANTIFUNGAL ANTIBIOTIC I. TAXONOMY OF THE PRODUCING STREPTOMYCETE AND ISOLATION OF THE ACTIVE PRINCIPLE*.
- Wang, Z., Oron, E., Nelson, B., Razis, S., & Ivanova, N. (2012). Distinct lineage specification roles for NANOG, OCT4, and SOX2 in human embryonic stem cells. *Cell Stem Cell*, 10(4), 440–454. <https://doi.org/10.1016/j.stem.2012.02.016>
- Wassink, T. H., Piven, J., & Patil, S. R. (n.d.). Chromosomal abnormalities in a clinic sample of individuals with autistic disorder. In *Psychiatric Genetics* (Vol. 11).
- Wong, C., Tavares-Ferreira, D., Thörn Perez, C., Sharif, B., Uttam, S., Amiri, M., Lister, K. C., Hooshmandi, M., Nguyen, V., Séguéla, P., Sonenberg, N., Price, T. J., Gkogkas, C. G., & Khoutorsky, A. (2023). 4E-BP1–dependent translation in nociceptors controls mechanical hypersensitivity via TRIM32/type I interferon signaling. *Science Advances*, 9(44), eadh9603. <https://doi.org/10.1126/sciadv.adh9603>
- Xiang, M., Gan, L., Zhou, L., Klein1ii, W. H., & Nathans, J. (1996). Targeted deletion of the mouse POU domain gene Brn-3a causes a selective loss of neurons in the brainstem and trigeminal ganglion, uncoordinated limb movement, and impaired suckling. In *Proc. Nati. Acad. Sci. USA* (Vol. 93).
- xiao2006. (n.d.).
- Yu, J., Vodyanik, M. A., Smuga-Otto, K., Antosiewicz-Bourget, J., Frane, J. L., Tian, S., Nie, J., Jonsdottir, G. A., Ruotti, V., Stewart, R., Slukvin, I. I., & Thomson, J. A. (n.d.). *Induced Pluripotent Stem Cell Lines Derived from Human Somatic Cells*. www.sciencemag.org
- Yu, Y., Yoon, S. O., Poulogiannis, G., Yang, Q., Ma, X. M., Villén, J., Kubica, N., Hoffman, G. R., Cantley, L. C., Gygi, S. P., & Blenis, J. (2011). Phosphoproteomic analysis identifies Grb10 as an mTORC1 substrate that negatively regulates insulin

- signaling. *Science*, 332(6035), 1322–1326.
<https://doi.org/10.1126/science.1199484>
- Yuan, H. X., & Guan, K. L. (2015). The SIN1-PH domain connects mTORC2 to PI3K. *Cancer Discovery*, 5(11), 1127–1129. <https://doi.org/10.1158/2159-8290.CD-15-1125>
- Zeineddine, D., Hammoud, A. A., Mortada, M., & Boeuf, H. (2014). The Oct4 protein: more than a magic stemness marker. In *Am J Stem Cells* (Vol. 3, Issue 2). www.AJSC.us/ISSN:2160-4150/AJSC0001509